

Advancements and challenges in wireless power transfer: A comprehensive review

Zhe Liu,¹ Tong Li,² Siqi Li,^{1,*} and Chunting Chris Mi^{3,*}

¹Department of Electrical Engineering, Kunming University of Science and Technology, Kunming 650500, China

²Department of Transportation Engineering, Kunming University of Science and Technology, Kunming 650500, China

³Department of Electrical and Computer Engineering, San Diego State University, 5500 Campanile Dr, San Diego, CA 92182, USA

*Correspondence: lisiqi@kust.edu.cn (S.L.); mi@ieee.org (C.C.M.)

<https://doi.org/10.1016/j.nexs.2024.100014>

BROADER CONTEXT

Since Tesla proposed the concept of wireless power transfer (WPT) in 1880s, WPT technology has transitioned from communication to energy transmission after more than 100 years of exploration and development in electromagnetics. It has gradually entered people's daily lives and industrial scenes, providing a convenient and flexible power supply for consumer electronics devices and industrial electronics applications. Since the beginning of the 21st century, with the increasing demand for electricity and the growing importance of energy management, WPT technology is expected to have huge potential and application value. This technology utilizes various methods such as magnetic fields, electric fields, microwaves, and lasers to achieve energy transmission under different high frequencies of electromagnetic waves. It has been extensively explored and demonstrated in various fields, such as consumer electronics, electric vehicles, implantable medical devices, solar space power stations, and aerospace; however, it still faces numerous challenges in practical applications. Therefore, this paper provides a detailed review of the physical mechanisms and resonance theories of WPT technology, performance enhancement methods, application scenarios, and future research directions, aiming to provide a comprehensive reference for relevant practitioners and researchers to promote the various applications of WPT technology in modern technology fields.

ABSTRACT

This paper provides a comprehensive overview of recent advancements, challenges, and potential applications of wireless power transfer technology. It covers various aspects of wireless power transfer, including magnetic-field coupling, electric-field coupling, microwaves, and laser technologies. The paper sheds light on physical mechanisms, current state-of-the-art techniques, their limitations, and the prospects of this rapidly evolving field, with a focus on both theoretical developments and practical implementations. This review aims to contribute to the understanding and advancement of wireless power transfer systems for diverse applications in the modern technological landscape. This paper discusses not only the field of wireless power transmission that has already been applied, such as wireless charging of electric vehicles, consumer electronics, implantable medical devices, and underwater equipment, but also applications that are still under research such as space microwave transmission, large-scale free space energy transmission, and roadway-powered electric vehicles.

INTRODUCTION

Wireless power transfer (WPT), inspired by Nikola Tesla's innovative concept in the 1880s, has evolved from conventional wired methods to become a vital, convenient, and safe technology in modern life.¹ Initially, WPT research focused on using microwave technology for long-distance applications like solar space power stations (SSPSs).² With the rise of electric devices, the demand for safety and convenience has surged, leading to significant advancements in WPT technology. Magnetic field coupling wireless power transfer (MC-WPT), known for its superior performance and design simplicity, is widely used in various industries, including electronics, medical implants, and electric vehicles (EVs).³⁻⁵

Technological limitations in batteries have forced electric devices to rely on battery replacement or increased capacity to meet prolonged operational demands, presenting challenges such as safety risks, additional weight, and higher initial costs.⁶ WPT technology offers a solution to these challenges. For instance, wireless charging for implantable medical devices (IMDs) reduces medical expenses and the risks associated with replacement surgeries.⁷ Implementing WPT infrastructure along roadways can address range limitations in EVs.⁸ In portable devices, wireless charging is now a standard feature, such as in modern smartphones, enhancing the convenience and intelligence of daily life through WPT.⁹ WPT has integrated into various aspects of life, and researchers are extensively exploring its mechanisms, performance enhancements, and diverse applications.¹⁰⁻¹³

Currently, WPT technologies are categorized into four types based on their mechanisms: MC-WPT, electric field coupling wireless

power transfer (EC-WPT), microwave wireless power transfer (M-WPT), and laser wireless power transfer (L-WPT).¹⁴⁻¹⁷ The overview diagram of the WPT system is illustrated in Figure 1. MC-WPT and EC-WPT, both near-field technologies, have their advantages and limitations. MC-WPT is relatively mature, offering adaptability, safety, and efficiency, but is limited by its short transmission distances and higher costs.¹⁴ EC-WPT, efficient at close range, is suitable for embedded systems but has shorter transmission distances and environmental sensitivity.¹⁵ Far-field technologies like M-WPT and L-WPT have their distinct challenges. M-WPT enables long-distance transmission but faces issues like energy loss and safety concerns.¹⁶ L-WPT is efficient and directional but requires high accuracy and faces atmospheric absorption and safety challenges.¹⁷

This paper provides a thorough overview of the latest developments, challenges, and applications of WPT technology. It elucidates the basic principles and applications of four WPT technologies, explores traditional analytical methods, novel physical concepts, and the role of electromagnetic metamaterials, and discusses the future trends and unresolved issues in WPT. The goal of this paper is to offer insights into WPT technology, fostering further research and development in this field.

Published by The Hong Kong Polytechnic University in association with Cell Press, an imprint of Elsevier Inc.

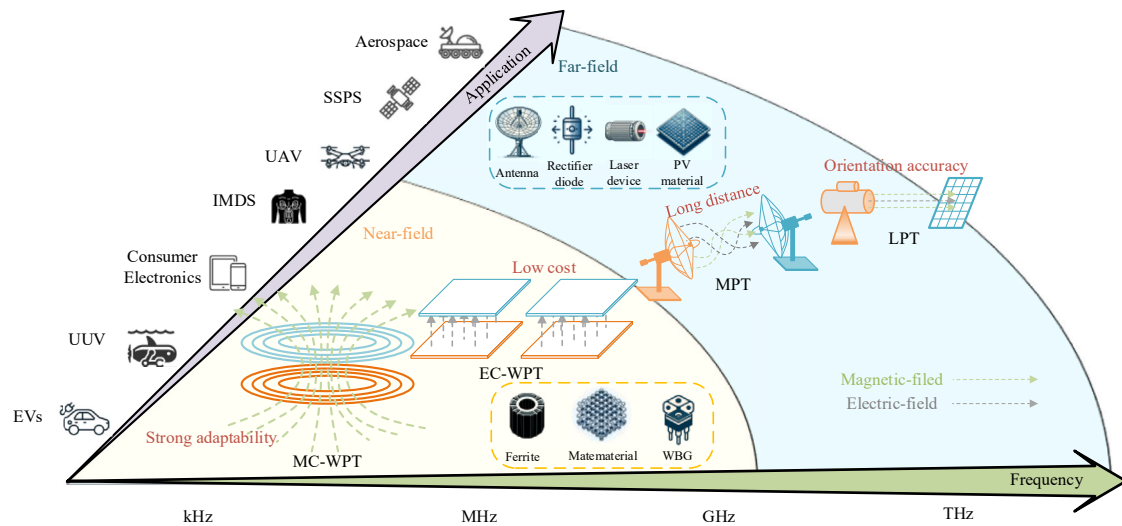


Figure 1. Overview diagram of a typical WPT system

PHYSICAL MECHANISM OF WPT

Unlike wired charging, which relies on wires for power transfer, WPT technology utilizes energy carriers such as magnetic fields, electric fields, microwaves, and lasers to achieve power transfer. This approach circumvents the drawbacks of tangled wires and potential safety risks inherent in wired power transfer, enhancing safety, convenience, and reliability. This section systematically explores and elucidates the physical mechanisms underlying diverse WPT technologies, comparing the advantages, disadvantages, and application scenarios of four different technologies.

Near-field WPT

Near-field WPT encompasses two primary categories: MC-WPT and EC-WPT, which utilize magnetic and electric fields, respectively, as the medium for energy transmission. These technologies have attracted considerable attention recently, especially for their enhanced reliability and safety in short-range WPT applications.¹⁵ Notably, MC-WPT technology stands out due to its high efficiency and technological maturity, leading to its widespread implementation and evolution into mature products across various applications.⁸ As an alternative to its magnetic counterpart, EC-WPT offers a lightweight coupling structure and high flexibility, positioning it as a potential technology in future WPT developments.¹²

Magnetic field coupling

In the field of MC-WPT systems, research typically categorizes the technology into two types: inductive wireless power transfer and magnetic resonant coupling WPT.¹⁸ Both methods utilize magnetic fields as the medium for energy transfer. Initially, MC-WPT studies did not incorporate compensation networks to enhance system performance. Energy transfer relied solely on magnetic induction between two coils, evident in early applications like wireless charging for electric toothbrushes.¹⁹ Contemporary research on MC-WPT focuses on improving transmission performance through various compensation networks and resonance mechanisms, optimizing parameters such as power, efficiency, and distance.²⁰

The structure of the MC-WPT system with two coils is depicted in Figure 2A, where inductor L_1 represents the transmitting coil, and L_2 the receiving coil. Initially, a 50-Hz grid AC power is converted to DC via an AC to DC converter with power factor correction. A high-frequency inverter then converts the DC voltage to high-frequency AC voltage, injected into the transmitting coil via a compensation network, generating an alternating magnetic field. The receiving coil induces an AC voltage, enhanced by a secondary resonance network for improved power factor, and a rectification circuit converts the high-frequency AC to DC, supplying power to the load or charging batteries.

Applying classical circuit theory and neglecting coil resistive losses, the active power from the primary side to the secondary side can be expressed as²¹

$$P_{MC} = \omega M_{12} I_1 I_2 \sin \varphi_{12}, \quad (\text{Equation 1})$$

where ω represents the angular frequency and $\omega = 2\pi f$, M_{12} is mutual inductance, I_1 and I_2 are the effective values of currents in the primary coil and secondary coil, and φ_{12} is the phase difference between the currents I_1 and I_2 . From Equation 1, it can be observed that when the phase difference between the voltages at the two ends is 90° , ie, $\varphi_{12} = \pi/2$, the system can achieve maximum power transfer.

The coupling coefficient between the transmitting coil and the receiving coil is defined as k_M , and

$$k_M = \frac{M_{12}}{\sqrt{L_1 L_2}}. \quad (\text{Equation 2})$$

The efficiency can be calculated when the system reaches a resonant state. R_1 , R_2 , and R_{eq} represent the resistances of the two windings and the equivalent load resistance, with $R_{eq} = 8R_L/\pi^2$. The quality factors Q_1 and Q_2 are defined as $Q_1 = \omega L_1/R_1$ and $Q_2 = \omega L_2/R_2$. Simultaneously, let $a = R_{eq}/R_2$, and the system's transmission efficiency can be determined as follows:

$$\eta(a) = \frac{1}{\frac{1}{a + \frac{1}{2}} + \frac{1}{k^2 Q_1 Q_2} + \frac{1}{a}} \quad (\text{Equation 3})$$

The maximum efficiency can be derived as follows when $a = (1 + k_M^2 Q_1 Q_2)^{1/2}$.²²

$$\eta_{\max_MC} = \frac{k_M^2 Q_1 Q_2}{\left(1 + \sqrt{1 + k^2 Q_1 Q_2}\right)^2} \quad (\text{Equation 4})$$

According to the maximum efficiency formula, the efficiency is jointly determined by the coupling coefficient and coil quality factors. Typically, k_M is application specific, so enhancing coil quality factors, Q_1 and Q_2 , is crucial for maximizing efficiency.

In the two-coil MC-WPT system, increased transmission distance reduces the coupling coefficient, decreasing efficiency, as shown in Equation 4. To extend transmission distance, a multi-relay coil method can be used, as shown in Figure 2B. Compared with two-coil systems, multi-relay

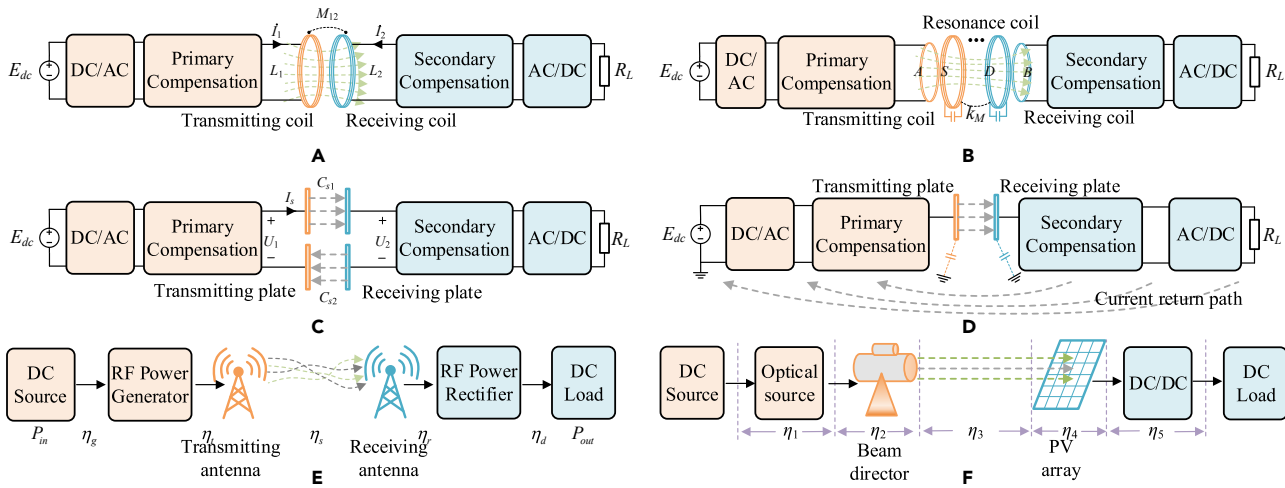


Figure 2. Physical mechanism of a typical WPT system

(A) Two-coil MC-WPT system. (B) Multi-relay MC-WPT system. (C) EC-WPT system. (D) Two-plate EC-WPT system. (E) M-WPT system. (F) L-WPT system.

systems maintain better performance by incorporating additional coils, aligning each coil's frequency with the system's resonance frequency. However, the extremely low coupling of long-distance transmission necessitates increased system frequency for effective energy transfer.

The four-coil MC-WPT system, a classic multi-relay example, achieved a 2-m transmission distance in 2007 using a self-resonant approach at MIT, which garnered considerable attention.²³ The transmission efficiency of this system, derived through coupled-mode theory, is given in Equation 5.

$$\eta_{\text{four-coil}} = \frac{(\Gamma_W/\Gamma_D)k_M^2/(\Gamma_S\Gamma_D)}{(1 + \Gamma_W/\Gamma_D)k_M^2/(\Gamma_S\Gamma_D) + (1 + \Gamma_W/\Gamma_D)^2}, \quad (\text{Equation 5})$$

where Γ represents the attenuation rate, subscripts S, W, and D denote source, load, and device, and k_M is the coupling coefficient between relay coils. The maximum efficiency is achieved when $\Gamma_W/\Gamma_D = (1 + k_M^2/\Gamma_S\Gamma_D)^{1/2}$.

Figure 3 compares the efficiency between two-coil and four-coil systems at varying distances.¹⁸ As distance increases, the four-coil system shows superior efficiency. However, in applications like EVs and mobile phone charging, requiring certain spatial constraints, multi-relay coils are less feasible. Therefore, research on multi-relay systems primarily targets scenarios like high-voltage power extraction from grids, and transferring energy from high-voltage lines to tower-mounted power supply equipment via insulators, as shown in Figure 4A.²⁴

Electric field coupling

EC-WPT technology can overcome the challenge of energy transmission blockages caused by metal obstacles and avoids eddy current losses. The coupling structures, typically made of metal, offer benefits such as simplicity, light weight, and low cost. Additionally, their shape can be flexibly designed for varied applications. Electric fields, sharing many similarities with magnetic fields and exhibiting duality in fundamental theory, make EC-WPT a potential area of research.^{25,26}

A typical EC-WPT system employs two pairs of metal plates as the coupling structure, as illustrated in Figure 2C. The DC power source undergoes high-frequency inversion, converting DC into high-frequency AC. This power is then boosted and impedance-matched through a compensating network, supplying the required high-voltage AC. An interactive electric field is established between the transmitter and receiver metal plates, inducing displacement current for energy transfer. The energy is further compensated and rectified to power the load. U_1 and U_2 denote the primary and secondary voltages of the coupler, and C_{s1} and C_{s2} are the capacitances between the metal plates. Disregarding cross-coupling capacitance and loss, the coupling capacitance C_s is determined as $C_{s1}C_{s2}/(C_{s1} + C_{s2})$, and the displacement current \dot{I}_s can be calculated as follows²⁷:

$$\dot{I}_s = j\omega C_s(U_1 - U_2 \cos \varphi_{21} - jU_2 \sin \varphi_{21}) \cdot \frac{\dot{U}_1}{U_1}, \quad (\text{Equation 6})$$

where φ_{21} is the phase difference between voltage \dot{U}_2 and \dot{U}_1 . Thus, the active power through the coupling capacitor is

$$P_{EC} = \omega C_s U_1 U_2 \sin \varphi_{21}. \quad (\text{Equation 7})$$

Equation 7 reveals that the transmission power of EC-WPT is directly proportional to the coupling capacitance C_s , frequency f , and phase difference φ_{21} , analogous to the MC-WPT system represented by Equation 1. The system achieves maximum power transfer at a phase difference of 90° ($\sin \varphi_{21} = 1$).^{28,29}

Cross-coupling capacitance between polar plates becomes inevitable with increased transmission distance and spatial constraints, forming six capacitances equivalent to a II-type circuit.³⁰ The coupling coefficient of EC-WPT is defined as

$$k_c = \frac{C_s}{\sqrt{C_1 C_2}}, \quad (\text{Equation 8})$$

where C_1 and C_2 are the equivalent self-capacitance of transmitting side and receiving side.

The system's efficiency under resonance is analyzed by introducing compensating networks. Let $b = G_{eq}/G_2$, where G_{eq} and G_2 are the conductance of the equivalent resistance R_{eq} and the secondary resonant circuit, respectively. The system's efficiency is then determined by²⁹

$$\eta(b) = \frac{1}{b + \frac{1}{b+2} + \frac{1}{k_c^2 Q_{C1} Q_{C2}} + \frac{1}{b+1}}, \quad (\text{Equation 9})$$

where Q_{C1} and Q_{C2} represent the quality factors of the primary and secondary circuits, respectively.

The system achieves maximum efficiency when $b = (1 + k_c^2 Q_{C1} Q_{C2})^{1/2}$.

$$\eta_{\text{max-EC}} = \frac{k_c^2 Q_{C1} Q_{C2}}{\left(1 + \sqrt{1 + k_c^2 Q_{C1} Q_{C2}}\right)^2} \quad (\text{Equation 10})$$

From Equations 4 and 10, the power and efficiency analyses of EC-WPT are similar to the conventional MC-WPT system.²¹ The two exhibit duality in basic theory and the fundamental principles are similar, allowing MC-WPT research methods and results to apply to EC-WPT, promoting its theoretical and practical applications.

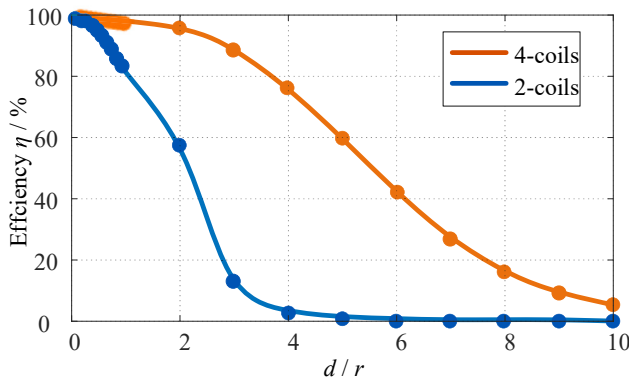


Figure 3. Efficiency between two-coil and four-coil systems at varying distances when $Q_1 = Q_2 = 1000$

The two-plate EC-WPT system uses two metal plates as couplers and the Earth as the return path, allowing energy transfer from the primary to the secondary, as depicted in Figure 2D. This method still employs an electric field as the transmission medium, using the self-capacitance of the coupling plates and stray capacitance to ground for a closed electrical circuit.^{31,32} For applications like EVs, the chassis' parasitic capacitance can act as a receiver plate, forming a closed circuit with the primary side.³³ Similarly, rail vehicles can use metal wheels and tracks as return paths.²⁷ This approach reduces costs, avoids cross-coupling issues, and provides a new solution for two-dimensional moving loads, as shown in Figure 4B.³⁴ However, this technology still needs more research, whose power levels and efficiency are not satisfactory for practical applications. Moreover, researchers need to explore more suitable application scenarios.

EC-WPT currently faces challenges such as low coupling capacitance, high voltage stress on the plates, and frequency limitations by wide-bandgap (WBG) devices, resulting in lower power density compared with MC-WPT.¹⁵ Increasing resonant frequency can enhance power density and reduce coupler size,³⁵ but its power level remains lower than MC-WPT,³⁶ mainly due to WBG device limitations at high frequencies.¹¹ Continuous improvement of WBG devices and ongoing research are expected to gradually address these challenges, given the strong demand for low-cost, flexible design solutions in practical applications.

Far-field WPT

M-WPT and L-WPT are far-field electromagnetic radiation technologies and utilize electromagnetic waves as carriers for energy transfer. However, during air transmission, they encounter interactions with other media, leading to medium losses and susceptibilities to scattering and refraction, which result in energy dissipation along the transmission path. Thus, M-WPT and L-WPT face challenges of low transmission efficiency and have been primarily used for signal transmission.^{37,38} Nevertheless, advancements in materials and technology have shown potential in improving their long-distance transmission efficiency. Both M-WPT and L-WPT technologies offer the capability to transmit energy to any point in space, garnering interest for long-distance WPT applications.^{39,40} European research groups have established a collaborative network focusing on this area through the European Cooperation in Science and Technology (COST) Project IC1301 on WPT for sustainable electronics.⁴¹ However, due to health concerns associated with high-power microwaves and lasers, future applications are frequently envisioned in unmanned environments or low-power scenarios. These include SSPSs, spacecraft, wearable devices, and the internet of things (IoT), as shown in Figures 4C and 4D.⁴¹⁻⁴³

Microwave

M-WPT employs microwaves, ranging from 300 MHz to 300 GHz, as a medium for energy transmission, facilitating WPT over considerable distances.⁴⁴ The system architecture is depicted in Figure 2E. A microwave power source converts electrical energy into microwave energy, which is then transmitted to the distant receiver via a transmitting an-

tenna. After traversing long-distance free space, the microwave energy is captured by a rectenna and converted into DC power for the load. Transmitting antennas are categorized into phased-array and directional antennas, often using a parabolic antenna structure for high-energy concentration. The rectenna comprises a receiving antenna, a low-pass filter, a rectifying diode, and a DC filter.

Efficiency is a crucial factor in quantitative analysis of microwave radiation-based WPT. The end-to-end power transmission efficiency of the M-WPT system can be defined as¹⁶

$$\eta_{MPT} = \frac{P_{out}}{P_{in}} = \eta_g \eta_t \eta_s \eta_r \eta_d, \quad (\text{Equation 11})$$

where η_g represents the efficiency of the direct current to radio frequency (DC-RF) converter, η_t denotes the efficiency of the microwave transmitting antenna emission, η_s is the free space transmission efficiency, η_r stands for the microwave receiving antenna efficiency, and η_d indicates the efficiency of the rectifying circuit conversion.⁴⁵ Power calculations in M-WPT are estimated using the path loss equation.⁴⁵ Microwave antenna design follows the Friis transmission formula, involving the microwave power source's output power determination and the gain calculation of the transmitting/receiving antenna based on the wavelength, transmission distance, and received power. The maximum received power is derived as follows⁴⁶:

$$P_{rm} = G_t G_r P_t \left(\frac{\lambda}{4\pi d} \right)^2 = \frac{A_t A_r}{\lambda^2 d^2} P_t, \quad (\text{Equation 12})$$

where P_t represents the transmit antenna power, G_t and G_r are the transmitting and receiving antenna gains, and A_t and A_r are their effective areas. While the distance d and operating wavelength λ are taken into account, the environmental attenuation that affects power is not considered in this estimation.

The efficiency of the energy emitter includes η_g and η_t . When considering a transmitter equipped with M antennas and operating at N frequencies f_n , where $f_n = f_0 + n\Delta f$ and the frequencies are evenly spaced by an intercarrier frequency spacing Δf , the transmit signal encompassing all M transmit antennas can be represented in vector form as follows⁴⁷:

$$\mathbf{x}_{rf}(t) = \sqrt{2} \Re \left\{ \sum_{n=0}^{N-1} \mathbf{x}_n e^{j2\pi f_n t} \right\}, \quad (\text{Equation 13})$$

where \mathbf{x}_n denotes the weight vector across the M antennas at frequency f_n , with each complex weight scalar used to adjust the magnitude and the phase of the sinewave on antenna M and frequency f_n .

The signal optimization module controls such adjustments to benefit from a joint waveform and active beamforming gain. To achieve high conversion efficiency η_g , efficient high-power amplifiers must be utilized, and the transmit signal may need to be adjusted by the signal optimization module to meet constraints on the peak-to-average power ratio. The transmission efficiency of microwave transmitting antennas η_t depends on the optimization design of the antenna, specifically the aperture field distribution design of the transmitting antenna. Microwave radiation has strong penetration efficiency in the atmosphere and is essentially lossless; however, it can be affected by weather conditions, with higher humidity and rainfall leading to lower transmission efficiency η_s .⁴⁸

The rectifying antenna is the receiving part of the M-WPT system, and its efficiency comprises η_r and η_d . The improvement of η_r is similar to that of η_t . The optimization design of η_d needs to consider various factors such as the characteristics of rectifying diodes, impedance matching, DC load, and suppression of higher-order harmonics. By designing the rectifying circuit appropriately, η_d can be optimized. Assuming the load of the rectifying antenna is R_L and the voltage obtained by the load is V_D , the efficiency of the rectifying antenna can be obtained as follows⁴¹:

$$\eta_r \eta_d = \frac{V_D^2}{P_{rm} R_L L_{pol}} \times 100\%, \quad (\text{Equation 14})$$

where L_{pol} represents the matching factor of the receive-transmit antenna. If both the transmit and receive antennas are linearly polarized

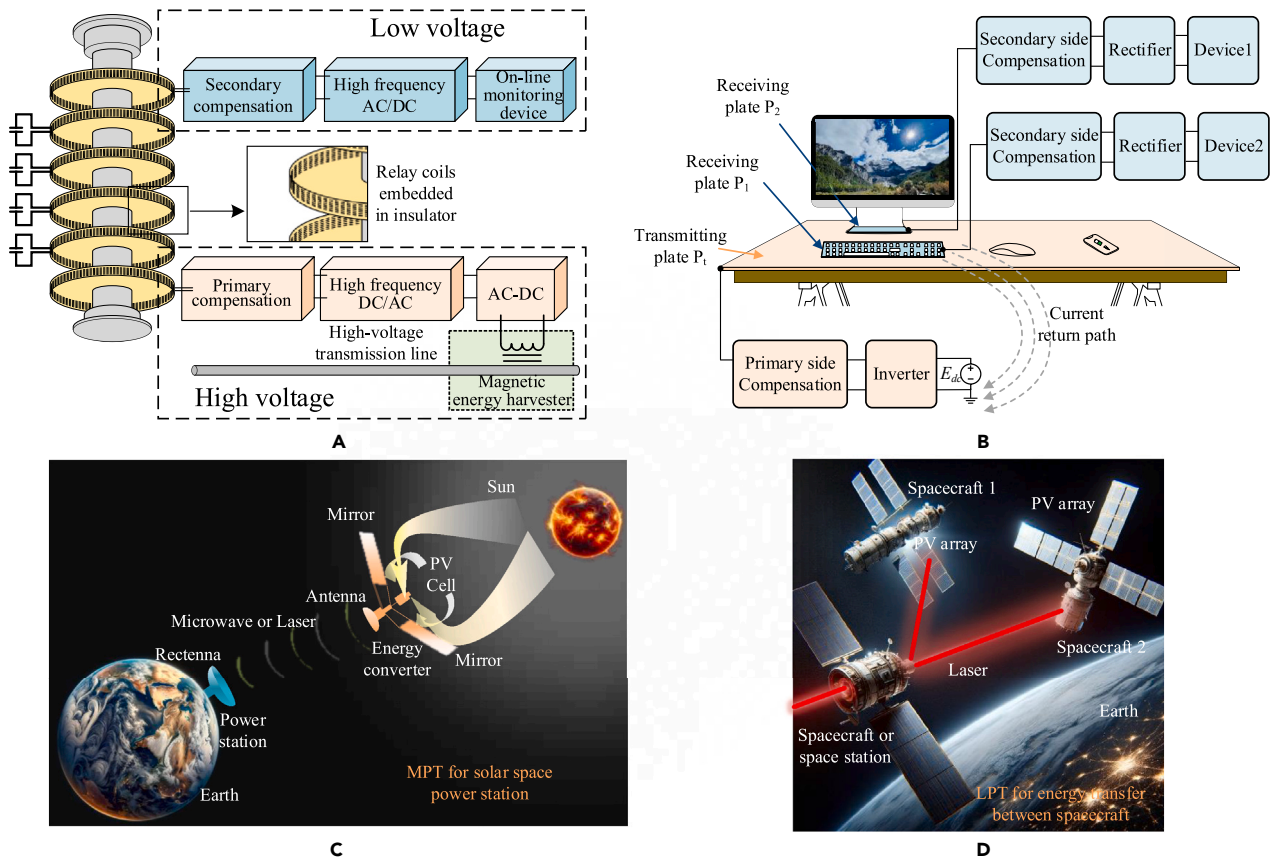


Figure 4. Potential application scenarios

(A) Multi-relay coils MC-WPT technology for energy harvester from high-voltage line. (B) Two-plate EC-WPT technology for desktop power supply. (C) M-WPT for solar space power station. (D) L-WPT for energy transfer between spacecraft.

or have the same circular polarization, indicating good alignment, then $L_{pol} = 1$. If the transmit antenna is linearly polarized and the receive antenna is circularly polarized, or vice versa, then $L_{pol} = 1/2$. Currently, the main bottleneck limiting the development of M-WPT technology is its relatively low transfer efficiency. To enhance the energy transfer efficiency of the system, extensive research has been conducted on high-power and efficient microwave power sources, efficient microwave rectifier devices, high-power and efficient rectenna arrays, as well as beamforming and beam control technologies.⁴⁹ Additionally, in practical applications, the negative impacts of high-power microwaves on biological safety and the ecological environment must also be considered.

Laser

Contrary to M-WPT, the L-WPT technology is based on the photoelectric effect, utilizing lasers as the energy transfer medium. Typically operating within the optical spectrum, L-WPT systems often employ infrared lasers, functioning in the range of several hundred terahertz (THz).⁵⁰ Figure 2F depicts the architecture of an L-WPT system. Here, electrical energy from the grid or a storage unit is converted into laser light by a laser power source. This laser light is then transmitted through an optical system and, after traversing free space, is captured by a photovoltaic (PV) array at the receiver, where it is reconverted into electrical energy. Optoelectronic conversion devices transform the laser's light energy into electricity, with subsequent rectification, voltage regulation, filtering, storage, and power supply to the load managed by an energy management module.⁵¹ L-WPT technology is characterized by its high-energy density, precise directionality, extensive transmission distance, and emission-reception aperture efficiency, rendering it ideal for innovative power supply solutions to mobile devices like sensors, aircraft, spacecraft, and space solar stations.⁵² Presently, L-WPT research is hindered by device maturity, atmospheric conditions, and tracking accuracy, affecting system energy transmission efficiency.

Figure 2F also illustrates the L-WPT efficiency breakdown diagram. The overall energy transfer efficiency of the system equals the product of each subcomponent's conversion efficiencies. The transmission efficiency of the L-WPT system is calculated as⁵³

$$\eta_{LPT} = \frac{P_{out}}{P_{in}} = \eta_1 \eta_2 \eta_3 \eta_4 \eta_5, \quad (\text{Equation 15})$$

where η_1 is the electro-optical conversion efficiency of the laser, η_2 is the efficiency of the laser, η_3 is the transmission efficiency of the laser in space, η_4 is the energy reception efficiency, and η_5 is the photoelectric conversion efficiency of the PV converter.

Assuming the distance between the laser and the target is R , the relationship between the radiation brightness L and the radiation intensity E of the laser satisfies the following equation⁴⁰:

$$E = \frac{\eta LS}{R^2} = \frac{\eta P}{R^2 \Omega}, \quad (\text{Equation 16})$$

where η represents the transmission efficiency between the laser output end and the target, and $\eta = \eta_2 \eta_3 \eta_4$. P is the power of the laser, and Ω is the divergence angle of the laser. It can be seen from Equation 16 that the parameter performance of the laser directly affects the system's conversion efficiency.

The typical choice for lasers is between semiconductor lasers and solid-state lasers. Generally, semiconductor lasers have slightly higher efficiency compared with solid-state lasers. Semiconductor lasers can adjust their power by regulating the current. The input voltage V for semiconductor lasers usually remains constant, so the electro-optical conversion efficiency can be represented as follows⁵⁴:

$$\eta_1 = \frac{\eta_d}{V} = \left(1 - \frac{I_{th}}{I}\right), \quad (\text{Equation 17})$$

Table 1. Comparison table of four typical WPT technologies

Method	Frequency	Distance	Efficiency	Advantages	Disadvantages	Application	Devices
MC-WPT ^{14,18,21}	Low frequency (kHz to MHz)	Medium range (mm to m)	High (up to 90%)	Simple structure, high safety, high efficiency	Limited distance, sensitive to misalignment, interference with other devices	Mobile phones, brushless motors, portable devices, wearable devices, EVs, UAV, UUV	Wire coils, WBG
EC-WPT ^{18,25,29}	Medium frequency (MHz)	Short range (mm to cm)	Medium (up to 80%)	Low cost, light, flexibly, low eddy loss, good misalignment tolerance	Limited distance, environmental impact, low power, potential electric field hazards	Implantable medical care, mobile phones, EVs, UAV	Metal plate, WBG
M-WPT ^{12,16,39}	Microwave band (MHz to GHz)	Long range (km to space)	Low (20%–40%)	Long distance, low atmospheric loss during transmission	Susceptible to atmospheric conditions, high cost, complex equipment, atmospheric attenuation	Spacecraft, satellites, SSPS, aircraft	RF antennas, phased arrays, rectennas
L-WPT ^{17,38,40}	Optical band (THz)	Long range (km to space)	Low (10%–15%)	Long distance, high directivity	Low safety, sensitive to atmospheric condition, low efficiency	UAV, SSPS, UUV, portable devices, moon rovers	Lasers, photocells, lenses, PV array

where i represents the laser's current, η_d is the laser's differential slope efficiency, and I_{th} stands for the laser's threshold current. It can be observed that for semiconductor lasers, higher input current leads to lower threshold current, resulting in higher electro-optical conversion efficiency.

The emission efficiency η_2 and reception efficiency η_4 primarily depend on the beam divergence rate and the absorption efficiency of PV cells. In long-distance transmission, reducing the laser's divergence angle is necessary to increase the transmission distance and minimize energy loss during laser transmission. However, for PV receivers, the beam size at the receiver location is relatively large after long-distance transmission, leading to energy loss. Therefore, designing the structure of PV receivers to reduce light reflection and increase the direct radiation area of the laser is an effective means to improve efficiency.⁵⁵

The attenuation of laser over longer transmission distances is mainly caused by the absorption and scattering of light by the transmission medium. When the laser undergoes long-distance transmission, the radiation intensity E on the target surface is given by⁵⁶

$$E = \frac{3.44P \exp(-\varepsilon L)}{\pi L^2 (\delta_d^2 + \delta_i^2 + \delta_j^2 + \delta_b^2)}, \quad (\text{Equation 18})$$

where P represents the laser power; L denotes the target distance; ε signifies the transmission medium's extinction coefficient due to absorption or scattering; and δ_d , δ_i , δ_j , and δ_b are the beam-spreading factors associated with diffraction, turbulence, beam jitter, and thermal blooming, respectively. Therefore, an increase in the beam-spreading factor due to environmental factors significantly reduces the radiation intensity on the target surface, thereby affecting the transmission efficiency η_3 . The PV conversion efficiency η_5 is mainly related to the wavelength of the laser and the power density of the incident laser. The conversion efficiency increases with the increase in power density. Additionally, temperature is also one of the important factors influencing the PV cell's conversion efficiency, which decreases as the temperature rises. The laser PV conversion efficiency can also be estimated based on the efficiency under solar spectrum.⁵⁶

$$\eta_5 = \eta_s \frac{P_{solar}}{J_{sc}} (QE) \frac{\lambda}{1240nm} \times \left[1 + \frac{25mV}{V_{oc}} \ln \left(QE \frac{\lambda}{1240nm} \frac{\varphi}{J_{sc}} \right) \right], \quad (\text{Equation 19})$$

where η_s is the photoelectric conversion efficiency of the solar, P_{solar} is the intensity of the solar, J_{sc} is the short-circuit current density under so-

lar, and V_{oc} is the open-circuit voltage under solar. φ is the intensity of the laser and QE is the internal quantum efficiency of the wavelength of the laser.

It can be observed that η_5 is not only related to the wavelength of the laser but also to the intensity of the laser. As the laser intensity increases, the photoelectric conversion efficiency continuously increases; however, when the laser intensity reaches a certain limit, the formula begins to fail.

Due to the small divergence angle and beam size, L-WPT has the potential to transmit high-intensity light over longer distances, providing unique advantages in certain applications, especially in IoT. For IoT terminals such as beacons, tags, and sensors, L-WPT is a promising alternative to traditional charging mechanisms, characterized by small beam size, good directionality, and long transmission distances.¹⁷ It can be integrated into 5G systems, forming a new network paradigm called wireless powered communication networks (WPCNs), which will pave the way for various research related to future overall system architecture.⁵⁷ In fact, the main challenge of WPCN will be adapting to low wireless power available over long distances, as well as the complexity of jointly transmitting wireless information and power on the same network, making L-WPT technology a very suitable solution.

However, current L-WPT technology faces challenges and limitations in terms of efficiency, safety, optical communication, beam collimation, and pointing accuracy. Efficiency is particularly crucial and remains one of the key issues that L-WPT technology needs to address. From the perspective of power transmission links, ensuring the conjugate image impedance at the WPT link ports is necessary to achieve optimal power transmission efficiency.⁵⁸ Additionally, to increase efficiency, in-depth research on the efficiency of PV cells is required to enhance the overall system efficiency.⁵⁹

Comparison

Table 1 presents a comparative analysis of the characteristics of four typical WPT technologies: MC-WPT, EC-WPT, M-WPT, and L-WPT. MC-WPT technology employs power electronics to convert energy and transfer it through loosely coupled transformers based on resonance principles. It boasts a simplistic implementation with the capability to transmit several hundred kilowatts and exhibits the highest efficiency. Its widespread applications include transportation, portable devices, and underwater robotics, benefiting from a straightforward structure, high safety, and efficiency. However, limitations include a limited transmission range, sensitivity to coupling alignment, and potential

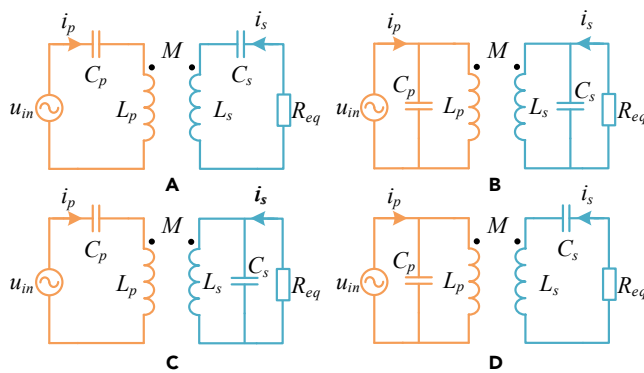


Figure 5. Basic compensation in MC-WPT
(A) SS. (B) PP. (C) SP. (D) PS.

interference with other devices.^{14,18,21} EC-WPT technology, known for its lightweight, thin, and cost-effective design, is utilized in short-range power supply scenarios like medical devices and consumer electronics. It operates by transferring energy through electric fields at high frequencies, reducing the impact of metallic obstacles. Nonetheless, its power output is constrained by the low dielectric constant of air, and it requires advancements in wide-bandgap devices.^{18,25,29} M-WPT technology, transmitting energy as microwaves through free space, faces transmission losses primarily from atmospheric conditions, dust particles, and obstructions. It can precisely control microwave beam intensity and direction, making it apt for space solar power stations and high-altitude aircraft. Its strengths include long transmission distances and low transmission losses, but its high cost and complexity limit its everyday use.^{12,16,39} L-WPT technology, transferring energy via lasers, offers strong directionality and energy concentration, suitable for unmanned aerial vehicles, solar power stations, and underwater applications. However, it is significantly influenced by environmental factors, and the potential health risks of lasers warrant further investigation.^{17,38,40}

Performance improvement

To augment the practicality and reliability of WPT technology, ongoing research efforts are dedicated to enhancing its performance. In near-field WPT systems, performance is contingent upon compensation networks, coupling structure design, as well as the converters and power control methods. For far-field WPT systems, advancements and improvements in devices, including generators and receivers, and the optimization of the entire system are crucial. Additionally, innovative analysis methods and the application of novel materials offer unique perspectives for further enhancements.

MC-WPT

To enhance the practicality and efficacy of MC-WPT systems, research has centered on refining compensation networks, coupling structures, converters, and power control methods. These elements are pivotal for improving misalignment tolerance, system efficiency, and output stability in MC-WPT systems.

Compensation network

The compensation network is designed not only to bring the system into resonance for maximizing power transfer capability but also to achieve load-independent output and other high-performance characteristics through judicious parameter configuration. Introducing compensation capacitors to the primary and secondary coils creates resonance with coil inductance, generating the necessary magnetic field.⁶⁰ On the primary side, compensation topologies minimize input apparent power,⁶¹ while on the secondary side, they counteract the inductor's reactive power to enhance transmission capability.⁶²

Depending on whether the compensation capacitor is in series or parallel with the transmitting/receiving coils, fundamental compensation methods include series-series (SS), series-parallel (SP), parallel-series (PS), and parallel-parallel (PP) configurations, as shown in Figure 5.⁶¹

These configurations enable zero-phase angle (ZPA) input for unit power factor. Dual topologies have been implemented to switch between parallel and series compensation on the secondary side, allowing constant current (CC) and constant voltage (CV) modes for battery charging.⁶³

High-order compensation topologies like LCL are gaining attention for their ability to alternate between constant voltage and current sources.⁶⁴ LCC compensation networks, adding a capacitor in series with the primary coil, are adjusted for zero-current switching (ZCS)⁶⁵ and can achieve unit power factor pickup on the secondary side.⁶² As a result, double-sided LCC compensation topologies have been proposed for resonance frequency and coupling coefficient independence from load conditions, maintaining zero-voltage switching (ZVS) conditions.⁶⁶ A variety of high-order compensation topologies have been analyzed for their constant voltage and current output characteristics.⁶⁷ Special topologies, such as S-N, are proposed for strongly coupled applications to integrate receivers into devices cost-effectively.⁶⁸

Hybrid compensation topologies are investigated to enhance misalignment tolerance, combining traditional configurations where one topology's output gain is proportional to mutual inductance, while the other's is inversely proportional. This design minimizes output fluctuations within a specific offset range.⁶⁹ To address the issue of a drastic increase in inverse current after the removal of the pickup, the SS and double-sided LCC topologies are connected in series to suppress system output power fluctuations to within 5%.⁷⁰ Although there are more diverse topology combinations that can be analyzed, these topologies require a careful balance between efficiency reduction and performance, as they involve the use of many components.⁷¹

Coil design

The design of the coupling structure is also a crucial pathway to enhance the misalignment tolerance, and its key lies in constructing a uniform magnetic field to ensure a relatively constant induced voltage. Such methods can be broadly categorized into two types based on coil structure: asymmetric coil structures and multi-coil structures. Asymmetric coil structures mainly achieve a relatively uniform magnetic field by increasing the coil size,⁷² optimizing coil parameters,⁷³ and utilizing helical coil structures,⁷⁴ ensuring a relatively stable induced voltage in the system. Multi-coil structures aim to enhance the misalignment tolerance of the system from both planar and spatial perspectives.

In multi-coil structures, efficiency and cost trade-offs are made for improved misalignment tolerance and multi-degree-of-freedom performance. Planar designs like double D (DD) coils increase effective charging areas, but require supplementary coils like Q-shaped ones for blind zones.⁷⁵ Cost-effective alternatives like bipolar pad (BP) coils achieve similar effects.⁷⁶ Employing a closely aligned multi-coil structure, the design parameters are optimally engineered to achieve mutual inductance decoupling. This approach enables the realization of a wireless power source characterized by high voltage, high isolation, and high power density.⁷⁷ To enable free movement of the pickup on the plane, multiple coils arranged in an array were suggested, creating a larger charging area, but the system efficiency is closely related to the number of loads.⁷⁸ Spatial designs propose multiple orthogonal coils forming a sphere or cylinder.^{79,80} This is a current research focus, as it can provide a power supply to multiple randomly distributed electronic devices within a space.⁸¹ With in-depth research into multi-degree-of-freedom systems, the electromagnetic field can not only effectively distribute in three-dimensional space but can also be directed and concentrated on the load by adjusting the magnetic field direction.⁸² However, the system still faces challenges, including limited spatial freedom, large coupling mechanism volume, mutual interference among multiple load receivers, and unreasonable power distribution. Addressing these issues will be a key focus of future research on multi-degree-of-freedom, multi-load WPT systems. Figure 6 shows the different coil types.

Converter and power control

Owing to the necessity for large inductors in current source converters, MC-WPT systems predominantly opt for half-bridge and full-bridge voltage source resonant converters. These systems, functioning in high-frequency ranges, have their power capabilities constrained by the characteristics of switching components, the topology of power

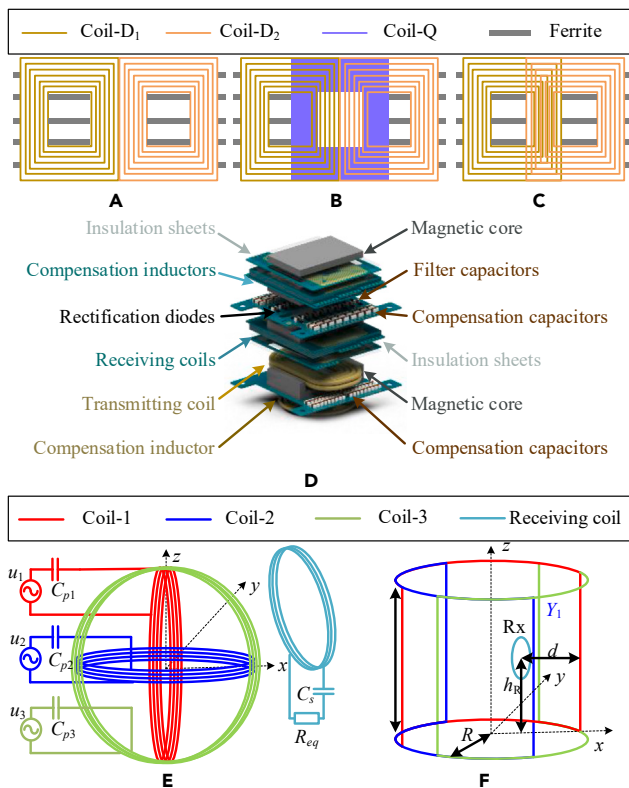


Figure 6. Different coil type

(A–C) DD pad, DDQ pad, and BP pad. (D) Wireless high-voltage power supply. (E and F) Sphere-type and cylinder-type.

electronic inverters, and associated control strategies.¹¹ A multi-phase parallel inverter was proposed to augment the WPT system's output power.⁸³ In a similar vein, an efficient 6-kW parallel MC-WPT power source topology was introduced aimed at reducing power-sharing imbalances due to component tolerances, thereby eliminating the need for extra reactive components.⁸⁴

In terms of control strategies, frequency, duty cycle, and phase shift are the primary methods employed.^{85,86} Frequency control necessitates consideration of bifurcation in scenarios with loose coupling, whereas in fixed frequency settings, duty cycle or phase shift adjustments are utilized for control.⁸⁶ Challenges with duty cycle or phase shift control include the risk of high cyclic currents in converters, potentially leading to the loss of ZVS or ZCS conditions. To maintain ZVS, another approach involves adjusting the input DC voltage.⁸⁷ An innovative asymmetric voltage cancellation method was proposed, which alters the duty cycle to increase the ZVS area.⁸⁸ Efficient control is key to optimizing transmission efficiency, adjusting the equivalent load impedance by modulating the output voltage and phase shift of the active rectifier.⁸⁹ A maximum efficiency point tracking (MEPT) scheme was proposed for closed-loop WPT systems to maximize energy efficiency under varying load and coupling conditions.⁹⁰ Last, a cost-effective MEPT approach was proposed that operates without power or current sensors, utilizing DC-DC converter control for load adaptation.⁹¹

EC-WPT

Similarly, the performance enhancements of EC-WPT systems depend on their compensation topology and coupling structure designs. Given air's low relative permittivity and practical size constraints on coupling metal plates, EC-WPT systems typically exhibit coupling capacitances in the picofarad (pF) range. This results in a high coupling impedance, significantly exceeding the load impedance. To facilitate efficient energy transfer, these systems operate at high frequencies, usually in the MHz range, and also lead to the need for faster control measures.

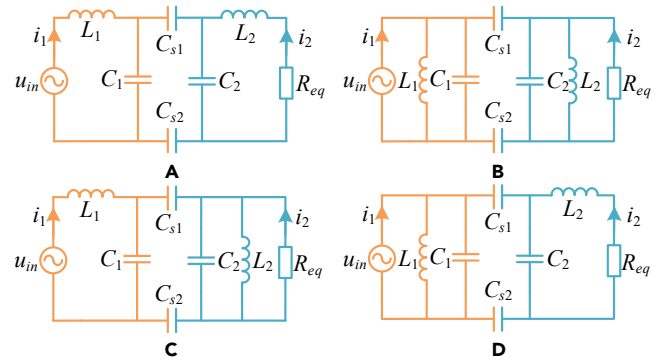


Figure 7. Basic compensation in EC-WPT

(A) SS. (B) PP. (C) SP. (D) PS.

Compensation network

The primary-secondary compensation network boosts voltage on the primary side plates while reducing it on the secondary side. This compensation topology not only adjusts the resonance frequency and increases misalignment robustness, but also ensures high efficiency and reduces converter power requirements.²⁹ The key challenge in EC-WPT systems is balancing minimal coupling capacitance with power needs. In short-distance applications, the coupling plates act as a capacitor, typically compensated by series inductors, forming an inductor compensation circuit on both the primary and secondary sides. The compensation inductor's value depends on the capacitor size and resonance frequency. To minimize the inductor, a very high resonance frequency is often necessary.⁹² Simplifying the secondary side, the two inductors can merge into one on the primary side.⁹³ This network is common in small air gap applications like biomedical devices and synchronous motors.^{94,95} To further reduce the value, size, and cost of the compensation inductor, an external capacitor can be connected parallel to both sides of the coupling structure.⁹⁶ Drawing from the four basic topologies of MC-WPT, EC-WPT adopts similar compensation networks, as depicted in Figure 7. Although simpler, these networks limit the control system performance improvement.⁹⁷ Recent research focuses on higher-order compensation networks to enhance performance and adjustable parameters. In this regard, Wang et al.⁹⁸ summarize and analyze the resonance conditions and stable output capabilities of four basic topologies and a series of higher-order compensation networks. The double-sided LCLC topology, an early higher-order network, directly links system power to the coupling coefficient; however, multiple compensation elements add cost and weight, reducing efficiency. For high-power needs, the LC-CLC topology enhances misalignment robustness and maximizes power output.²⁸ Addressing mobile device flexibility, a Z impedance-based circuit prevents high-voltage peaks on sudden secondary-side removal.⁹⁹ An F-type network protects MOSFETs from damage,¹⁰⁰ and a double-T network avoids voltage and current shocks, enabling standby mode.¹⁰¹

For longer distances, the impact of cross-coupling capacitance requires viewing the structure as six capacitors formed by the four plates. Two-port network theory simplifies this to a behavior source model or a II-type circuit. The equivalent capacitance also serves as compensation, reducing passive components. Thus, the double-sided LCLC simplifies to an LCL.³⁰ An LCL-L network reduces secondary-side components.¹⁰² For dynamic charging in rail vehicles, a stacked MC-WPT system with four coils ensures constant current output.²⁷

Metal plate design

EC-WPT systems use metal electrodes, typically copper or aluminum, as coupling structures, classified into parallel and stacked types. Initial research focused on parallel structures with two electrode pairs. To mitigate cross-coupling, these were spaced apart or made larger than the transmission distance,¹⁰³ but it limited range and increased space requirements. Placing parallel plates closer enhances cross-coupling effects but decreases coupling capacitance, necessitating higher system frequencies and additional compensation for resonance.¹⁰⁴ The stacked structure, more compact and misalignment-tolerant, suits

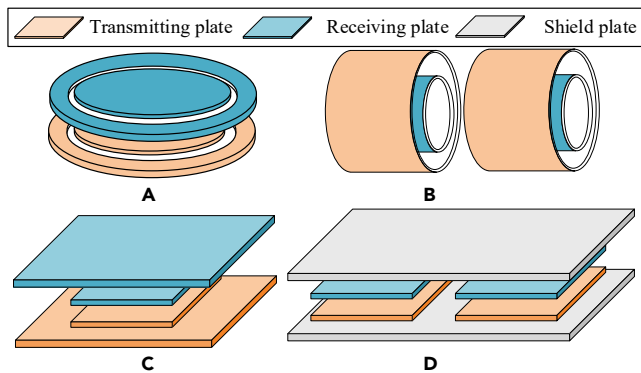


Figure 8. Different coupling structure with EC-WPT
(A) Disc type. (B) Sleeve type. (C) Stacked type. (D) Six-plate type.

mobile devices powering in confined spaces.³⁰ An interleaved capacitive coupler was developed to improve mutual capacitance.¹⁰⁵ However, high-power applications suffer from electric field leakage. Adding a metal plate on each side of the two parallel plates, forming a six-plate structure,¹⁰⁶ improves shielding. In EVs, two additional plates can be replaced by the car chassis and ground. Metal's plasticity allows diverse shapes like disc or cylindrical structures for applications like slip rings or brushless motors,¹⁰⁷ overcoming regular replacement issues in mechanical slip rings. For mobile device free-positioning, a stacked array structure and a well-designed receiver ensure stable power delivery.¹⁰⁸ An interdigital electrode capacitive coupler maintains 5-W power under horizontal and vertical movement.¹⁰⁹ A multi-load stacked structure achieves free-positioning for multiple devices on a two-dimensional plane, outperforming coil-based MC-WPT systems in cost and flexibility.³⁴ However, higher voltage levels in coupling structure raise concerns about leakage electric field radiation, necessitating further research. Figure 8 shows the different coupling structure with the EC-WPT system.

Converter and power control

Due to the duality between EC-WPT and MC-WPT systems, the coupling structure is the main difference between the two technologies. With relative permittivity and practical size constraints and results in smaller coupling capacitance, the EC-WPT systems necessitate drive frequencies above MHz. Therefore, the converter of the EC-WPT system typically employs half-bridge, full-bridge, and Class-E configurations. Meanwhile, MC-WPT systems also expect to operate with the MHz range in current research to minimize the size and weight of the coupling structure.¹¹⁰ The research on converters for both technologies is almost consistent.

Research on the control of EC-WPT systems primarily revolves around enhancing performance under variations in coupling capacitance and equivalent load. This involves power flow control and tuning control. Buck converters are utilized at both the transmitter and receiver ends to adjust the system's output voltage and current.¹¹¹ To track the system's resonance frequency, adjustable inductors and capacitor matrices are employed to tune the system to the resonance point during parameter drift, ensuring stable output.¹¹² Employing a multi-loop control approach combining frequency adjustment and variable inductance allows for the tracking of the system's resonance frequency using a phase-locked loop structure. By adjusting the variable inductance to adapt to changes in the compensation network, this method effectively controls the output power under variations in coupling capacitance.¹¹³ Similarly, combining frequency control with phase adjustment enables effective tracking of the system's constant voltage frequency, maintaining system stability.¹¹⁴

M-WPT

A primary challenge in M-WPT systems is balancing the size and efficiency of the transmitting and receiving antennas. Enhancing transmission efficiency necessitates enlarging the transmitting antenna's aper-

ture for more focused microwave power or increasing the receiving antenna's aperture for improved energy capture. However, antenna aperture sizes are restricted by practical applications, adversely affecting long-distance transmission efficiency. Additionally, the dispersion of radiofrequency energy in the environment complicates M-WPT systems. The receiving antenna must be compact yet efficient, and capable of broadband, multi-frequency, wide-angle, and polarization-independent reception. These multi-faceted requirements pose significant complexities in designing antennas for M-WPT systems.

Transmitter

The transmitter of an M-WPT system comprises two primary components: the power source and the transmitting antenna. The power source utilizes four types of components: magnetrons, traveling-wave tubes, multi-beam klystrons, and GaN solid-state power devices.¹¹⁵ Currently, GaN devices are prevalent due to their high efficiency, high breakdown voltage, and robustness in harsh environments.¹¹⁶ However, GaN devices produce significant harmonics in the output power within the microwave frequency range due to nonlinearity. These harmonics can reflect power and reduce efficiency.¹¹⁷ Harmonic control circuits, such as class-F mode, one of the most efficient power amplifier circuits, are employed to mitigate this issue.¹¹⁸ Recent studies have also focused on reverse class-F (class-F⁻¹) mode, featuring ideal interchangeability between current and voltage output waveforms.¹¹⁹

The transmitting antenna serves two main functions: direction tracking and positioning, and focusing. Beam-tracking control achieves direction tracking and positioning.¹²⁰ The antenna array automatically tracks moving receiving devices using pilot signals after phase-array processing. For optimal microwave energy transmission, sidelobes of the transmitting antenna are minimized, and characteristic beamwidth is maintained to reduce spillage loss. Addressing microwave scattering caused by antenna array structures, two high-precision phase control methods, position and angle correction, and the parallel method, have been suggested. These methods limit phase deviation to less than 1°. Optimal focusing is achieved by feeding the conditional antenna array and designing an appropriate network.^{39,122} Uniform feeding schemes are commonly used in transmitting antenna arrays. For instance, a large-scale radiation structure with uniformly weighted radiation modules was implemented, successfully transmitting 20 W of RF power over 150 km.¹²³

Rectenna

Efficiency improvement in rectennas is crucial for the overall efficiency of M-WPT systems. The rectifying diode, the core component of the rectifying circuit, has seen performance advancements with new materials. Efficiency has progressed from early semiconductor Si diodes to Si Schottky diodes, and then to GaAs Schottky diodes, reaching about 80%.¹²⁴ To further enhance rectifying circuit efficiency, impedance-matching networks are designed to match the rectifying and front-end circuits. M-WPT receivers utilize various rectifier types with different topologies, and numerous models have been proposed.¹²⁵ However, rectifying device nonlinearity in the microwave band causes impedance changes due to power, frequency, and load variations, impacting rectifier performance and M-WPT receiver efficiency.¹²⁶

Active circuit methods have also been employed to optimize rectification efficiency. A Class-E RF rectifier based on a reconfigurable Class-E power amplifier circuit delivered 50 mW of DC power at 900 MHz with 83% efficiency.¹²⁷ Time-domain duality theory was applied to demonstrate rectifier construction by reversing power flow from load to DC power.¹²⁸ Further studies on RF rectifier topologies using time-domain duality aimed to increase conversion efficiency and power levels for high-frequency applications. This rectifier used ideal RF chokes, ideal DC isolators, and lossless transmission lines, with source impedance conjugately matched with rectifier input impedance at varying input power levels.¹²⁹

Combination array

To enhance power levels in M-WPT, single rectifying antenna units are insufficient, and arraying is necessary. The main arraying schemes include the combination of individual rectifiers, sub-array combinations, and rectenna arrays, as shown in Figure 9.¹³⁰ The individual rectifier combination architecture is characterized by high efficiency due to the coherent summing of impinging power.¹²⁹ However, it has

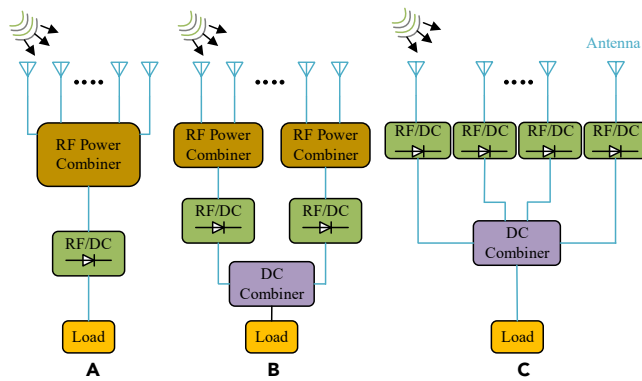


Figure 9. Architectures of M-WPT receiver

(A) RF power combined first then rectified. (B) Partial RF power combined and then rectified. (C) RF power rectified first then DC combined.

drawbacks, such as low robustness and challenges in obtaining high-power diodes. To mitigate these, a sub-array combination architecture was proposed. For example, a dual-rhombic loop antenna sub-array at the RF level was created by grouping four folded dipole antennas, duplicated, and combined in DC to form a 4×16 receiving array, achieving 82% collecting efficiency.¹³¹ Rectenna arrays offer simplicity but yield lower overall efficiency compared with coherent reception. A large rectenna array with 2,304 units achieved a maximum output of about 600 W and 50% efficiency.¹³² A vertically stacked rectenna array with four layers and 16 rectifying units per layer showed that DC power from the four-layer stack was five times that of a single layer.¹³³

L-WPT

L-WPT technology has the lowest efficiency among the four techniques. However, laser technology benefits from a reduced mass and volume—approximately 10% of comparable microwave devices. Its high energy density renders it particularly suitable for military weapon development and space applications. Nevertheless, laser transmission through the atmosphere is significantly affected by atmospheric conditions, prompting research focus on enhancing both laser emission and PV reception technologies to improve overall system transmission efficiency.

Laser

L-WPT systems primarily utilize two types of lasers: solid-state and semiconductor lasers.⁵⁶ Semiconductor lasers, or laser diodes (LDs), are a mature, rapidly evolving technology characterized by small size, lightweight, long lifespan, and high efficiency. LD efficiency at kilowatt levels typically ranges between 45% and 60%.¹³⁴ However, their output beam quality is suboptimal, impacting energy density at the receiver and making them suitable mainly for short-distance, low-to-medium-power L-WPT systems. Solid-state lasers, using light for excitation and solid materials for laser generation, can produce output powers up to tens of kilowatts, fitting high-power, long-distance L-WPT systems.¹³⁵ Their electrical-to-optical conversion efficiency, ranging from 20% to 30%, is comparatively low due to indirect excitation through a pump source. Beyond laser types, key advancements in laser emission technology include beam collimation and shaping. Techniques like a Keplerian telescope system for beam divergence reduction and collimation,⁵¹ and a pinhole lens for beam splitting, superimposing, and intensity distribution uniformization have been developed.¹³⁶

PV receivers

The PV receiver, fundamental to reception technology of L-WPT, aims to enhance PV array efficiency by altering its geometric shape. Flat-panel PV receivers offer simplicity, ease of processing, low cost, and straightforward tracking. Nevertheless, they require high uniformity in laser irradiation, with non-uniform irradiation potentially causing significant energy loss.¹³⁶ Building on flat-panel designs, a serrated array PV panel was proposed to ensure equal irradiance across all units, as depicted in Figure 10A.⁴⁰ However, laser beam reflection by cell angles reduces power transmission to PV cells, challenging efficiency improvement in PV receivers.¹³⁷ To mitigate non-uniform irradiation effects on PV-to-electric conversion efficiency, a PV cavity converter was developed,

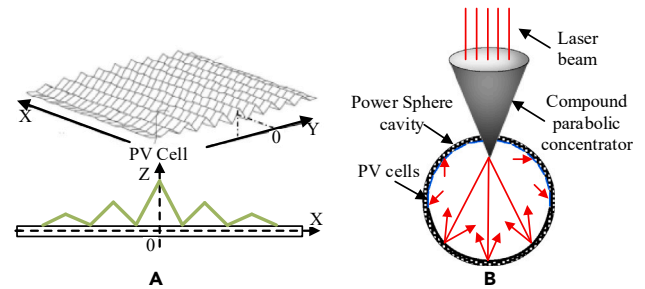


Figure 10. Different PV receiver geometries

(A) Sawtooth configured array. (B) PV cavity converter.

which efficiently converts high-density laser energy into electricity, as shown in Figure 10B, but require high precision in laser beam incident angle due to concentrator aperture limitations. Convergent-type PV receivers use Fresnel lens to intensify laser beams on PV cells, increasing PV-to-electric conversion efficiency and potentially reducing receiver cost.¹³⁸ However, these receivers are more complex, heavier, and have strict incident angle requirements.

MPPT

Laser light's inherent Gaussian distribution results in non-uniform irradiance on PV arrays, increasing mismatch losses and reducing peak power. The power-voltage characteristics of PV arrays also display multi-peak features, rendering traditional maximum power point tracking (MPPT) methods ineffective.¹³⁹ A two-step approach introduces MPPT technology based on equivalent load-lines.¹⁴⁰ Under uneven illumination, this method adjusts the array's operating point to the intersection of the optimal load line and the array's current-voltage curve. Traditional perturbation observation methods then move the operating point to the global maximum power point. Further, intelligent control methods like particle swarm optimization and artificial bee colony algorithms were employed, facilitating adaptive, accurate global maximum power point searches under varying array structures and irradiance conditions.¹⁴¹

Novel concept of WPT

In recent research, the WPT field has seen the emergence of innovative physical concepts, notably the theories of PT-symmetry and coherent perfect absorption (CPA), offering fresh perspectives on enhancing the transmission performance of WPT systems. By harmonizing system gain and loss, PT-symmetry significantly enhances the robustness of efficiency. Additionally, the unique electromagnetic properties of metamaterials and metasurfaces, achieved through strategic structural design, endow WPT systems with superior physical characteristics compared with natural materials, showing exceptional promise in boosting efficiency, extending transmission distances, and improving electromagnetic shielding.

PT-symmetry and CPA

First introduced in 1998 by Carl M. Bender and Stefan Boettcher in quantum mechanics, PT-symmetry posits that non-Hermitian systems can exhibit real eigenvalues under parity and time-reversal symmetry.¹⁴² This is mathematically represented by the commutation of parity and time-reversal operators with the Hamiltonian, denoted as $[PT, H] = 0$, with P and T representing parity and time-reversal operators, respectively.¹⁴³ Extending beyond its quantum origins, PT-symmetry has gained traction in classical wave systems, including optics, photonics, and electronics.¹⁴⁴⁻¹⁴⁶ Systems with PT-symmetric structures, a unique non-Hermitian class, adeptly balance gain and loss. A key PT-symmetry phenomenon is the exceptional points (EPs), where scattering matrix poles merge on the real frequency axis in non-Hermitian active systems, resulting in degenerate, non-orthogonal eigenfunctions.¹⁴⁷

In near-field WPT systems, PT-symmetry theory addresses the challenge of maintaining transmission efficiency and power output amidst variable coupling and loads. The MC-WPT system's transmitter incorporates a nonlinear saturated gain negative resistance, crafted using operational amplifiers, as the gain element for the PT-symmetric system.

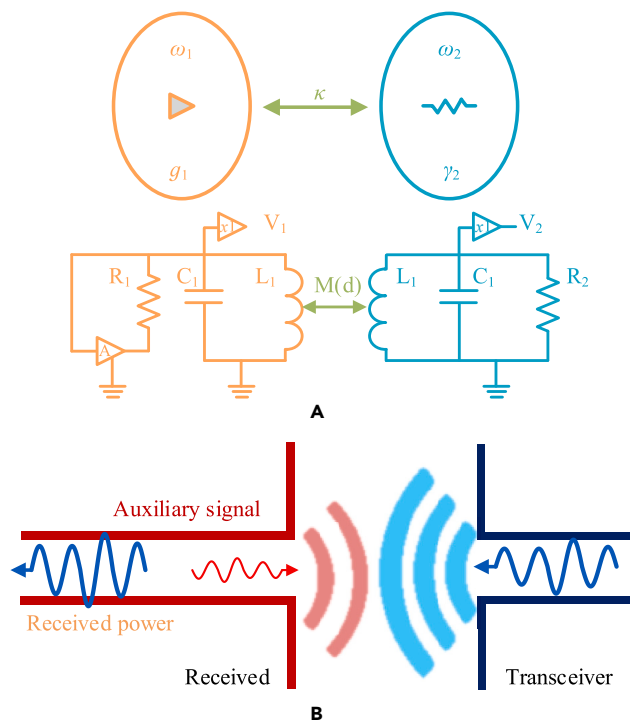


Figure 11. Novel concept of WPT
(A) PT-symmetry. (B) Coherent perfect absorption.

This allows for efficient energy transfer across a broad range. For instance, within about 1 m, transmission efficiency remains stable,¹⁰ as shown in Figure 11A. Expanding on this, an omnidirectional WPT system is applied in unmanned aerial vehicles (UAV), achieving stable output power with approximately 93.6% transmission efficiency.¹⁴⁸ The introduction of a power-efficient switch-mode amplifier with current sensing feedback in an odd-even-time symmetric circuit ensured robust, efficient wireless power transmission, maintaining stable power output and high efficiency.¹⁴⁹ Despite these advancements, PT-symmetry in WPT systems faces limitations such as increased complexity, reduced power range, and heightened noise sensitivity.¹⁵⁰

In M-WPT, through self-oscillation facilitated by nonlinear active components, the system autonomously establishes a steady state, enabling robust operation against environmental or load position variations.¹⁵¹ However, negative resistors used in such configurations can introduce parasitic losses, necessitating careful design to maintain system efficiency and stability.¹⁵² By finely tuning gain and loss interactions in oscillation cavities, stable single-frequency microwave oscillation is achievable without optical/electrical filters.¹⁵³

CPA conceptualized as the time-reversed counterpart of lasers allows for the complete absorption of pure incident radiation modes by lossy media. CPA functions as linear absorption interferometers, useful in applications like detectors, transducers, and switches, as shown in Figure 11B.¹² The utilization of EPs in lasers introduces novel functionalities for tailored applications in specific laser and sensing domains.¹⁵⁴ Under laser threshold, active systems facilitating EPs tend to become nonlinear and irreversible in their cutoff phase,¹⁵⁵ offering new possibilities for WPT applications. Recent advances in PT-symmetric optics have led to practical applications in laser systems operation, optical isolators, CPA lasers, and single-mode lasers.^{156–158}

Metamaterials and metasurfaces

Metamaterials, artificial composites with periodic or non-periodic microstructures, offer revolutionary properties not seen in natural materials. By intricately arranging small crystal cells, these materials can have their effective permittivity or permeability adjusted to positive, near-zero, or negative values. This allows metamaterials to exhibit unique characteristics, such as negative refraction, inverse Cerenkov radiation,

and inverse Doppler effects, in specific frequency ranges.¹⁵⁹ Metamaterials are categorized based on their effective permittivity ϵ and permeability μ into four types: conventional double-positive (DSP), epsilon-negative (ENG), mu-negative (MNG), and double-negative (DNG) materials, as shown in Figure 12A.¹⁶⁰

Metamaterials often involve complex arrangements of metallic wires and structures, demanding advanced manufacturing techniques. Metasurfaces, the surface version of metamaterials, are created by arranging electric scatterers or voids in two-dimensional patterns on surfaces. They offer more compact structural possibilities compared with three-dimensional metamaterials. Both metamaterials and metasurfaces hold potential to enhance the efficiency, operational distance, and misalignment tolerance of near-field WPT systems. Additionally, rectangular antennas based on metamaterials can achieve higher RF-DC current conversion efficiency.¹⁶¹

In near-field WPT research, metasurfaces have been shown to improve transmission efficiency, distance, and enhance misalignment resistance.¹⁶² A comprehensive review of metamaterial and metasurface-based WPT systems was introduced, considering various dimensions and configurations.¹⁶³ Metamaterials in WPT systems help focus, shield, or guide electromagnetic waves.¹⁶⁴ A common method to enhance WPT performance involves focusing electromagnetic waves, typically by inserting a metasurface between the transmitter and receiver, as shown in Figure 12B.¹⁶¹ In systems with two coils, metasurfaces can be modeled using a magnetic dipole approach.¹⁶⁵ The effective magnetic permeability control of metasurfaces is crucial, and theoretical studies have explored near-field metasurface superlenses.¹⁶⁶ Metasurfaces are often non-uniform, with central units designed differently from edge units to allow direct magnetic field passage.¹⁶⁷ Efficient WPT systems using metasurfaces with cubic high-dielectric resonators have shown improved performance.¹⁶⁸ Placing a metasurface at the system's back end reflects electromagnetic waves and enhances coupling.¹⁶⁹

Positioning a metasurface with near-zero magnetic permeability on the WPT system's back minimizes electromagnetic field leakage, and placing it on the side can shield leakage and improve misalignment tolerance.¹⁷⁰ Metasurfaces can also shield edge fields in capacitively coupled WPT systems, reducing-edge electric fields and improving efficiency.¹⁷¹ Dynamically adjustable metasurface elements enable mobile devices to benefit from the metasurface at any position.¹⁷² Metamaterials and metasurfaces are crucial in powering medical implants and wearable devices, reducing electric field exposure, and providing safe wireless power.¹⁷³

In far-field WPT systems, metamaterials and metasurfaces are mainly used at the receiving end for beamforming and perfect electromagnetic energy absorption.¹⁷⁴ While antenna arrays are commonly used for beamforming,¹⁷⁵ they often face cost and complexity issues. Metamaterials and metasurfaces can adjust incident wave amplitude, phase, and polarization, and therefore, offer simpler alternatives.¹⁷⁶ Recent studies have integrated metasurfaces with near-field focusing in RF and mid-near infrared applications.¹⁷⁷ Reflective metamaterials and metasurfaces, such as multifocal reflective metasurface, enable varying reflection phase shifts, achieving high NFF transfer efficiency.

Application of WPT

Due to the ability of WPT technology to overcome the limitations of traditional wiring and demonstrate remarkable flexibility and safety, it has garnered widespread attention across various industrial sectors. A plethora of WPT products and demonstrative applications have rapidly emerged in diverse industries. Subsequently, we first review the array of standards for existing WPT systems, followed by a detailed investigation into the current state of research in WPT technology within several exemplary application domains, including EVs, consumer electronics, IMDs, and specialized industrial applications.

Standard

The development of WPT technology is accompanied by the establishment of a series of standards aimed at ensuring the safety, compatibility, and efficiency of the technology. These standards not only facilitate the widespread application of WPT technology but also provide

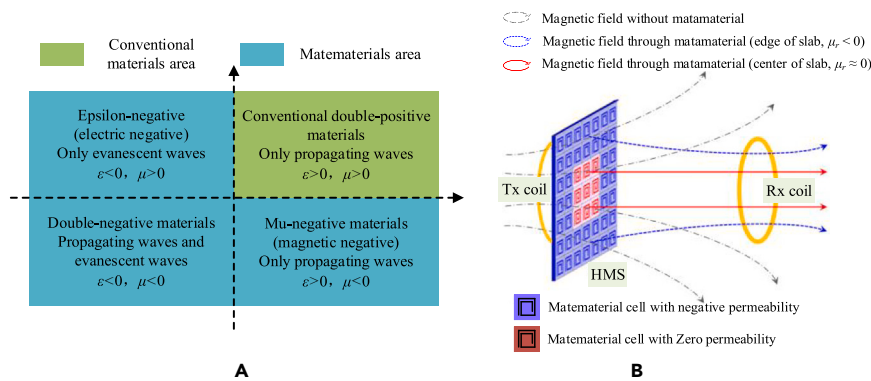


Figure 12. Matamaterial classification and examples

(A) Matamaterial classification. (B) Conceptual configuration of the WPT with the metamaterial slab.

clear guidance and frameworks for manufacturers, researchers, and consumers. The following are some of the main WPT standards that play a key role in various fields and applications.

Various standards, including Qi,¹⁷⁸ Airfuel Alliance,¹⁷⁹ Institute of Electrical and Electronics Engineers (IEEE),^{180,181} International Electrotechnical Commission (IEC),¹⁸² and Society of Automotive Engineers (SAE),¹⁸³ play vital roles in regulating WPT technology. These standards ensure safety, compatibility, and efficiency across different applications. Qi, established by the Wireless Power Consortium, focuses on small power devices like smartphones and tablets. The Airfuel Alliance, formed by merging A4WP and PMA, promotes broader interoperable wireless charging solutions. IEEE standards offer technical guidance for wireless charging systems, particularly in consumer electronics and portable devices. IEC standards, specifically IEC 61980, address safety and performance requirements for wireless charging systems in EVs. SAE standards, notably SAE J2954, provide a unified framework for EV wireless charging, emphasizing safety and interoperability.

Table 2 summarizes the scopes of different standards, outlining their technology types, application ranges, transmission distances, and relevant characteristics. Some standards focus on specific areas, such as the Qi standard targeting consumer electronics and SAE focusing on EVs, while others cover a broader range, including MC-WPT and radio frequency, such as Airfuel Alliance and IEC. IEEE standards for WPT mainly concentrate on wireless personal area networks.

Electric vehicles

The application of WPT in EVs eliminates the need for physical connectors and charging cables, offering a more convenient and efficient charging experience. The application can be divided into wireless charging of road vehicles and off-road vehicles.

For road vehicle applications, it can be further divided into two types: Roadway-powered electric vehicles (RPEVs) and stationary-charging electric vehicles (SCEVs). While stationary wireless charging eliminates the need of cable and plug, dynamic roadway charging enables charging infrastructure embedded in roadways, allowing continuous charging while an EV is in motion, hence, removing the need of physical charge stations. The application of RPEVs extends the range of EVs, particularly for heavy-duty and public transportation.

SCEVs

In application scenarios of SCEVs, the MC-WPT and EC-WPT technology are two commonly used methods due to the high power demand of EVs. The research about the EC-WPT for SCEVs is mainly focused on the compensation network, coupling structure, and E-field analysis. The introduction of double-LCLC compensation topology aids in enhancing system power.⁹⁶ The stacked-type coupling structures could decrease installation space.³⁰ Increasing operational frequency and optimizing compensation networks effectively boost power density, reduce voltage stress between couplers, and subsequently minimize electric field leakage.¹⁸⁴ Strengthening coupling capacitance by utilizing the metal enclosure at the vehicle's front as a receiving electrode plate, thus efficiently enhances system transmission power and field constraints, as shown in Figure 13A.¹⁸⁵ However, EC-WPT technology remains theoretical in its application to EVs due to issues like electric field leakage and limitations of high-frequency WBG devices.

Presently, MC-WPT technology can essentially meet the charge requirements of SCEVs, and several automobile manufacturers, such as BWM and SAIC, have equipped certain EV models with WPT systems. To enhance the flexibility and robustness of MC-WPT technology in SCEV applications, extensive research has been conducted on compensation networks, vehicle-to-grid (V2G), coupling structure design, and foreign object detection technology. The LCL compensation topology enables constant current output and unity power factor.⁶⁴ Building on this, an additional capacitor forms the LCC compensation network. The double-sided LCC network ensures that the resonant frequency is independent of coupling coefficients and load conditions and achieves ZVS conditions in power converters, making it the preferred choice for SCEV applications.⁶⁶ The use of bidirectional compensation networks, synchronized control technology, and power control strategies allows for bidirectional power flow between DC sources and energy storage devices, transforming EVs into mobile energy buffers and facilitating wireless interaction between the grid and EVs.¹⁸⁶ Rational coil structure and magnetic core arrangement design enhance system robustness and energy efficiency. The designs of DD, DDQ, and BP coils increase lateral misalignment tolerance and effective charging area.^{75,76,187} The integration of compensating inductors with magnetic couplers using magnetic integration methods enhances misalignment tolerance.¹⁸⁸ High magnetic permeability materials like ferrite and aluminum plates are used for magnetic flux guidance and shielding, effectively improving magnetic field density and reducing magnetic flux leakage.⁶⁴ Different magnetic core arrangements ensure efficiency stability while minimizing core material usage, as illustrated in Figures 13B–13E.¹⁸⁹

Foreign object is a significant challenge in SCEV applications.^{190,191} During the charging process, metal objects and living beings exposed to the magnetic field produced by the coupler may pose potential safety risks and adverse symptoms, making the detection of metals and living animals an essential consideration for commercial applications. Effective detection of metal foreign objects and living states is possible through the use of sensors, system parameters, and sensing modes. The design of various types of detection coils, installed on the coupler, and monitoring changes in open-circuit voltage or impedance in these coils can detect the presence of metal objects, as shown in Figures 13F–13L.¹⁹⁰

Despite advancements in MC-WPT and EC-WPT for SCEVs, challenges like efficiency, safety from electric field leakage, and the high-frequency demands requiring WBG persist. Integration into existing infrastructure, cost, and foreign object impact also pose hurdles. Addressing these through innovation is vital for the broader adoption of SCEVs.

RPEVs

RPEVs are becoming the most promising candidate for future transportation because they are ideally free from large, heavy, and expensive batteries, and get power directly while moving on a road. RPEVs have not been widely used so far due to the high initial investment cost for commercialization. As a solution for future intelligent travel, the WPT system for RPEVs is currently in the stage of prototype development and demonstration engineering construction.⁹

By employing MC-WPT technology, utilizing a single coil as a track would lead to exorbitant costs and reduced safety. Therefore, the long power rail is divided into multiple short power rails to selectively turn on power rails when RPEVs are on the power rails, which could be effectively reducing EMF on the track.¹⁹² Additionally, the use of auxiliary coils, power sources, and controllers can generate opposing magnetic flux to neutralize EMF.¹⁹³ Proper compensation network design can minimize electromagnetic interference (EMI) and reduce system power

Table 2. WPT standards

Standards	Technology type	Application range	Typical power output	Transmission distance	Compatibility	Frequency range	Main features
Qi ¹⁷⁸	Magnetic induction	Smartphones, tablets	Up to 15 W	Short range	Wide	Low frequency (<1 MHz)	Widely used, supports multiple power levels
Airfuel Alliance ¹⁷⁹	Magnetic resonance, radio frequency	Various devices	Variable	Medium to long range	Moderate	Wide range	Supports larger areas and multi-device charging
IEEE ^{180,181}	High-frequency wireless	Personal electronic devices	Variable	Short to medium range	Specific applications	High frequency (>2 MHz)	Focused on WPAN
IEC ¹⁸²	Various	Including EVs	Variable	Variable	Wide	Wide range	Emphasizes safety, efficiency, international compatibility
SAE J2954 ¹⁸³	Magnetic induction	EVs	Variable	Short range	Specific vehicle models	Low to mid frequency	Unified technical framework for EVs charging

loss to the maximum extent.¹⁹⁴ EC-WPT, as a potential technological solution, employs the metal chassis of track vehicles and metal tracks as the two plates of a coupler to realize dynamic EC-WPT, as shown in Figure 14A.²⁷ EC-WPT has advantages in misalignment tolerance and cost-effectiveness but is currently limited by power levels and low dielectric constants, requiring compensation through ultra-high operational frequencies, dependent on the further development of WBG devices.²⁶

Due to the oil crisis of the 1970s, the United States initiated some projects to investigate the WPT system for RPEVs in an effort to minimize vehicular oil usage.^{195,196} However, commercialization was not achieved due to issues like small air gaps, large lateral tolerances, and EMF problems. With advancements in devices and materials, WPT solutions for RPEVs have gradually become commercially viable. In 2010, the SAE established the SAE J2954 wireless charging working group to develop comprehensive standards for SCEVs.¹⁸³

In recent years, Korea Advanced Institute of Science and Technology (KAIST) has advanced research on the on-line electric vehicles (OLEV) project, achieving an operational efficiency of 83% at an output power of 60 kW, with a large air gap of 20 cm and a favorable lateral tolerance of 24 cm, leading to its first commercialization on a 48-km route in Gumi, South Korea.⁸⁷ Additionally, OLEV buses have been newly commercialized on two 12-km bus routes in Sejong, South Korea, as illustrated in Figure 14B.⁹ A significant European demonstration project named FABRIC was conducted in France and Italy by a consortium of European companies and research institutes.¹⁹⁷ In Guangxi, China, a 54-m dynamic WPT demonstration project was established. This project utilized a dual-transmitter and dual-receiver structure to reduce the number of inverters used and applied a magnetic integration scheme to increase power density, achieving 60-kW power and 87.5% efficiency with a 20-cm air gap, as depicted in Figure 14C.¹⁹⁸

As the core component of WPT technology, the magnetic coupling structure is the focal point of research in current RPEV demonstration projects. The design of the magnetic coupling structures determines several practical considerations in these projects, including cost (such as inverter quantity, road layout costs, and maintenance expenses), system transmission efficiency, misalignment tolerance performance, and electromagnetic radiation. Currently, magnetic coupling structures of RPEVs are mainly divided into two types: array type and rail type. The rail type includes transverse magnetic flux and longitudinal magnetic flux types, while the array type is further categorized into single-stage and bipolar types. Additionally, rail-type structures can also utilize multi-phase structures to suppress output voltage fluctuations.

Early demonstration projects typically used single-phase transverse magnetic flux rail-type coupling structures due to their simple structure and low construction costs. However, the inefficiency caused by the

entire rail operating simultaneously, and increasing electromagnetic radiation above the coupling structure with power levels were significant drawbacks.^{192,199,200} To improve transmission distance and power density, recent demonstration projects have adopted longitudinal magnetic flux rail-type structures and multi-phase structures for transmitting rails.^{201–203} Nevertheless, efficiency and radiation issues persist. Array coupling structures are commonly employed in current demonstration projects due to their high efficiency and low radiation levels.^{198,204–208} However, they necessitate significant initial construction costs, including a substantial number of inverters and position detection devices. Moreover, output fluctuations can arise from continuous switching processes.

The summary of the magnetic coupling structures used in implemented projects is presented in Table 3. Therefore, the commercialization of RPEVs involves a balance of factors such as cost, output performance, and safety, which is also the focus of future research. However, it cannot be denied that RPEVs remain an effective alternative to current EV charging methods. After all, compared with the initial costs and maintenance expenses of WPT tracks, reducing the number of batteries carried by road EVs also holds significant appeal.

This illustrates that multiple countries have demonstrated significant interest in RPEVs and have engaged in pertinent research efforts. The authors believe that the early adoption of roadway charging will be public fleets, such as buses and yard tractors. Public fleets benefit from reduced downtime, ensuring vehicles remain operational with minimal disruption. Furthermore, WPT will be an enabler for future autonomous vehicles and share mobility with automatic charging. The applications of WPT in EVs represent a transformative shift in charging infrastructure, offering a glimpse into a future where charging is seamless, automated, and integrated into various aspects of transportation systems.

RPEVs face challenges such as high initial costs, embedding charging infrastructure complexity, and EMF safety concerns. Issues like selective power rail activation and the need for precise vehicle alignment complicate dynamic charging systems. Current EC-WPT limitations in power and efficiency, alongside material and device technology needs, call for innovation, cost reduction, and policy support to make RPEVs a feasible future transportation solution.

Consumer electronics

Currently, WPT technology is widely used in various consumer electronic products, such as electric toothbrushes, smartwatches, and mobile phones. The MC-WPT technology for low-power electronic devices has become relatively mature. However, the current demand for miniaturization and lightweight in consumer products has led to limitations in the transmission distance of MC-WPT systems, and the need for precise coil alignment during charging, which lacks spatial freedom. Consequently, there is an increasing demand for free-positioning WPT systems in consumer electronics charging.²⁰⁹

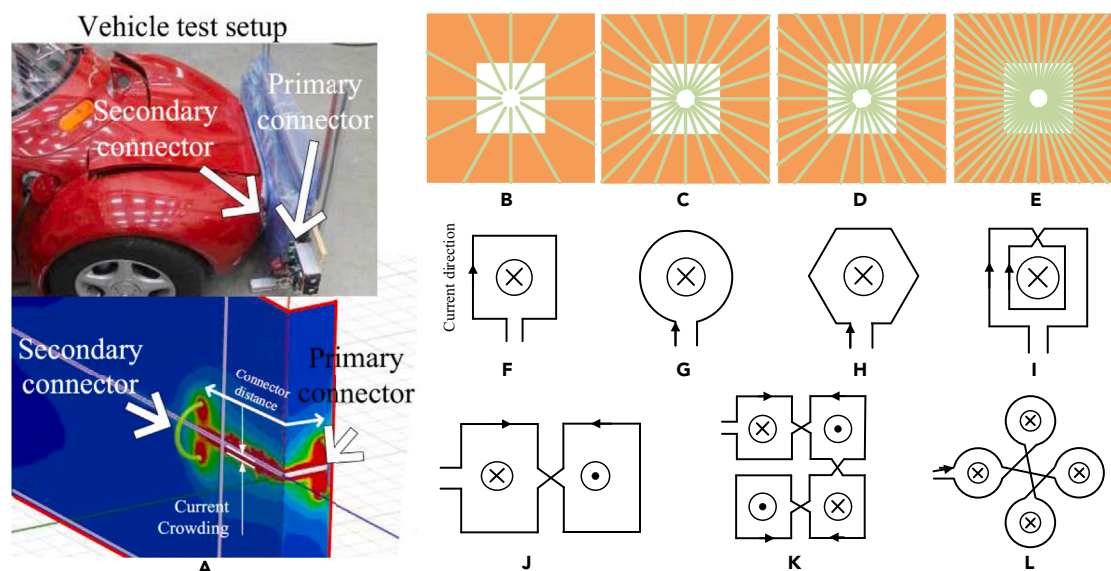


Figure 13. WPT in SCEV application

(A) EC-WPT technology in SCEV and the current path FEA simulation results. (B–E) Magnetic core layout method. (F–L) Different types of detection coils.

In WPT technology, the method of achieving free-positioning functionality by using multiple overlapping coils to form a transmitting coil has been researched and applied, as shown in Figure 15A.²¹⁰ Utilizing non-overlapping or shaped coils (eg, triangles, squares, hexagons) for flexible positioning, and anti-parallel winding stabilizes coupling factor variations, enhancing free-position stability.²¹¹ Metasurface technology has also shown the potential to enhance the efficiency of free-positioning WPT systems.²¹² Comparatively, EC-WPT systems have a cost advantage. Implementing rational coupling plate design, and two-plate EC-WPT technology can achieve effective free-positioning, as illustrated in Figure 15B, but their efficiency still requires enhancement.^{34,108,109}

Uniform magnetic field distribution within a specific spatial range can be controlled to provide a more flexible wireless power supply solution for consumer electronic devices. This is categorized into two-dimensional and three-dimensional omnidirectional WPT methods.²¹³ In three-dimensional omnidirectional WPT, various miniaturized couplers,⁷⁹ or cavity couplers designed within the device,⁸⁰ can supply power in the device's surrounding environment. Conversely, two-dimensional omnidirectional WPT, suitable for limited spaces like desktops, utilizes a three-phase magnetic field for uniform power distribution to multiple mobile devices.⁸²

The ideal goal of WPT technology is to achieve free-positioning WPT within a certain spatial range, liberating from the constraints of wires. As such, large-space WPT technology has long been a public aspiration. Using multi-mode quasi-static cavity resonance technology, a transmission efficiency of 37.1% was achieved in an 18-m³ room. Under safety standards, it is projected to deliver over 50 W of power, as depicted in Figure 16A.²¹⁴ A dual-loop large-space WPT system in a 25-m³ space delivered around 40 W of power with more than 30% efficiency, adhering to human electromagnetic safety standards, as demonstrated in Figure 16B.²¹⁵

Additionally, distributed laser charging (DLC) can effectively transmit energy in larger spaces. Using DLC, approximately 2 W of power was delivered over a 10-m distance, suitable for charging smartphones and laptops simultaneously. Two wireless charging network architectures were proposed: a DLC-assisted infrastructure-based network and a DLC-based self-organizing network, highlighting its potential for mobile device power supply.⁵² Resonant beam charging (RBC) technology, demonstrated for IoT devices, achieved 2 W of power at a 2.6-m distance.²¹⁶ However, as a potential WPT technology for IoT, L-WPT faces safety and efficiency challenges.

WPT technology, especially MC-WPT, has significantly advanced in consumer electronics, enabling wireless charging for devices like smartphones and smartwatches. Despite progress, challenges in miniaturization, transmission distance, and coil alignment limit charging freedom. Innovations in free-positioning systems, omnidirectional WPT, and methods like DLC and RBC offer solutions for more flexible and efficient charging across various devices. However, safety and efficiency remain key concerns, highlighting the need for further research and development.

IMDs and wearable devices

For IMDs, harnessing energy from the human body and its surrounding environment can ensure extended device longevity and reduce the costs and complications associated with battery replacements. WPT technology, as a power supply solution for IMDs, not only enhances flexibility²¹⁷ but also facilitates bidirectional communication, aiding in continuous external monitoring and treatment.²¹⁸

MC-WPT is a mature technology for IMDs, suitable for subcutaneous implants and deep-body medical devices. Based on the operating frequency, MC-WPT systems in IMDs are classified into near-field and mid-field types.²¹⁹ In near-field WPT systems, considerable research has focused on improving power transfer efficiency to IMDs. For instance, an enhanced Helmholtz coil was developed for uniform magnetic field generation, offering stable power to robotic capsules and increased transmission efficiency through a hybrid resonance method.²²⁰ Addressing the miniaturization needs of body implants, a WPT system based on flexible three-dimensional dual coils was proposed for small implantable devices, optimizing coil design and parameters.²²¹

However, near-field MC-WPT technology, due to its exponential decay characteristic, is less suitable for powering miniaturized devices deep within the body. Mid-field MC-WPT technology addresses this limitation but with lower efficiency. Considering specific absorption rate (SAR) constraints, the design using high-Q receiving coils and large external transmitting coils was optimized, effectively powering millimeter-sized free-floating implants within a large three-dimensional space, as illustrated in Figure 17A.²²² The viability of mid-field wireless powering was explored for transferring power to electronics located along the gastrointestinal tract, achieving received power levels of 37.5 μ W, 123 μ W, and 173 μ W in the esophagus, stomach, and colon of tested animals, respectively, while keeping radiation exposure below safety thresholds.²²³

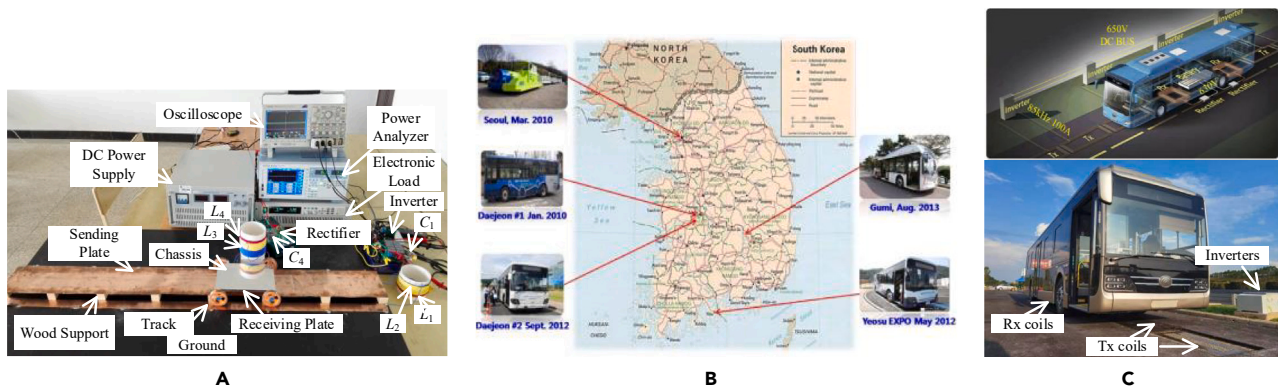


Figure 14. Implementation of RPEVs

(A) Dynamic EC-WPT system for railway application. (B) Deployment status of OLEVs in Korea. (C) Demonstration engineering construction with dynamic wireless charging in China.

For IMDs, EC-WPT technology must improve transmission performance by increasing electric field strength and frequency. Incorporating the flexibility of metal electrodes, a metal flexible patch was used as an electrode, attaining 35% efficiency and 2-mm implant depth at 130 MHz, with a total patch area of about 400 mm².⁹³ A novel EC-WPT technology application for powering deep-body implanted devices was proposed, as shown in Figure 17B.²²⁴ This approach employed a stacked coupling structure with intermediate plates as receivers and outer plates as transmitters, delivering 10-mW output power at 6.78 MHz. Since EC-WPT relies on electric fields for energy transfer and generates electric currents, minimizing such currents is essential to enhance transmission efficiency.²²⁵

For wearable devices, extensive research has been conducted with the far-field WPT. By embedding matrix antenna devices within garments, wireless communication between body sensor units can be achieved, as illustrated in Figure 17C.⁵⁸ All conductive components of the antennas are fabricated using nonwoven, low-cost adhesive fabrics, mitigating issues of wear and tear, thus allowing for intricate geometric designs. Moreover, within the context of 5G, leveraging heterogeneous, multi-radio small cells presents an opportunity for efficient WPT in wearable devices, enabling energy autonomy for IoT participants.²²⁶

WPT technology in IMDs and wearable devices faces challenges like efficiency, simultaneous wireless information and power transfer (SWIPT), especially in deep-body implants, and safety due to electromagnetic exposure. Future research must optimize designs and materials for safer, more efficient power transfer in IMDs and wearable devices.

Special industrial application

In numerous applications, WPT is required to be conducted with human safety considerations. However, in areas like underwater devices, oil-field drilling, and aerospace, these safety concerns can be relaxed to focus on optimizing transmission performance in specialized environments. Research in these industrial fields is expanding the scope of WPT, offering more flexible and convenient energy solutions for diverse sectors.

Underwater vehicles, particularly unmanned underwater vehicles (UUVs), face energy supply challenges that limit continuous operation. Traditional methods of energy replenishment, such as returning to shore or using wired connections, involve energy wastage, operational complexity, high costs, and connector deterioration. WPT technology offers a safer and more efficient solution. High-power UUVs typically employ MC-WPT and EC-WPT technologies. The primary challenge of MC-WPT technology under water is reduced efficiency due to increased eddy current losses. Research efforts have been dedicated to calculating these losses and proposing equivalent circuit models to enhance transmission efficiency.²²⁷ Other studies have focused on designing coupling structures tailored to UUV shapes, addressing system offset


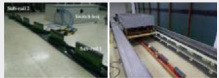


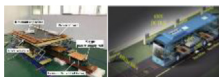
issues caused by undercurrents, as shown in Figure 18A.²²⁸ MC-WPT applications in actual waters have been experimentally validated, as depicted in Figures 18B and 18C.^{229,230}

EC-WPT technology's major hurdle under water is seawater's high electrical conductivity, complicating power transmission.²³¹ Studies have shown that increasing transmission frequency and exposing the plates can improve system efficiency, albeit with increased voltage breakdown risks.²³² Recent research achieved a 5-kW power transfer over 60 mm with 87.2% efficiency using a mixed medium approach in EC-WPT.²³³ The dielectric constant of water, 81 times that of air, significantly boosts EC-WPT's coupling capacitance, aiding power transmission in underwater environments. Yet, current research primarily focuses on pure water, and the impact of seawater on EC-WPT systems requires further exploration.

In rotary steerable drilling, harsh conditions such as high temperatures, pressures, vibrations, and liquid convection pose challenges to traditional wired transmission and brush slip rings. WPT technology offers a more efficient solution for energy and signal transmission in these environments.²³⁴ Designing a rotary coupling structure that maintains system performance during rotation is a significant challenge. MC-WPT systems, using circular coils or solenoids, can meet rotational requirements. An S-N topology was proposed to minimize secondary compensation and optimize core layout, reducing the cost of rotary coupling structures.²³⁵ A DD-type rotary WPT system with rotor state recognition was proposed, although it faces coupling coefficient zero points during rotation.²³⁶ To overcome this, a DD-4D double-layer orthogonal coil design was introduced for improved anti-offset capabilities.²³⁷ In EC-WPT technology, designing rotary coupling structures with metal plates is simpler and cost-effective.¹⁰⁷ However, liquid convection during drilling processes can cause significant changes in coupling capacitance, necessitating stable output solutions under drastic capacitance variations.

In aerospace, WPT is essential for powering drones and SSPSs for extended periods. Near-field WPT is primarily used for endurance enhancement of micro-drones and powering spacecraft solar wings,^{235,237} while far-field WPT enables long-distance power transmission, such as transmitting solar-generated electricity to ground receivers via microwave technology.² Early demonstration projects of M-WPT were primarily focused on powering drones. Dr. Brown, with funding from NASA, was the first to use silicon diodes as rectifiers to improve the efficiency of M-WPT systems. By incorporating diodes into the antenna array through light detection programs, the transmission power was enhanced. This successfully powered a small helicopter for 14 h of normal flight, as shown in Figure 19A.²³⁸ Additionally, Japanese researchers conducted experiments on microwave-lifted aircraft (MILAX), where they designed phased-array antennas and generated 2.411 GHz microwave energy to power aircraft models. The transmission array antenna was installed on a moving vehicle, and a lightweight

Table 3. RPEVs comparison of characteristics of magnetic coupling mechanisms for demonstrative projects

Type	M-Field type	Phases num.	Demonstration projects	Costs and difficulty	EM radiation	Output fluctuations	Distance	Eff.	Summary
Rail type	Transverse magnetic flux	Single phase ^{192,199,200}		★	★★★	Stable	★	★	● Simple control ● Small output fluctuations ● Low cost ● Low efficiency ● High EM radiation
	Longitudinal magnetic flux	Single phase ^{192,201}		★★☆	★★☆	★★☆	★★★	★☆	
		Multi-phase ^{202,203}		★★☆	★★☆	★	★★★	★☆	
Array type	Single	Single phase ²⁰⁴⁻²⁰⁷		★★	★★	★★	★	★★	● High efficiency ● Low EM radiation ● Complex control
	Bipolar	Single phase ^{198,208}		★★★	★	★ (Transverse) ★★★ (Longitudinal)	★★	★★★	● High cost ● Large output fluctuations

★ The more items listed, the more prominent the corresponding characteristics.
☆ Represents half of ★.

rectangular antenna with microstrip antennas was developed to demonstrate the ability to control microwave power beams toward moving targets, as shown in Figure 19B.²³⁹

The success of M-WPT technology in drone demonstration projects boosted researchers' confidence. It led to proposals like the SSPS

plan to address future energy issues, with a detailed feasibility analysis of SSPS. Japan showed strong interest in this technology and conducted numerous experiments and demonstration projects to improve M-WPT's transmission distance, efficiency, directional accuracy, etc., as shown in Figure 19C.²⁴⁰ Extensive research was also conducted on hardware subsystems in the SSPS system.²³⁹ The Japan Aerospace Exploration Agency (JAXA) transmits guiding signals from the receiving antenna side to the transmitting antenna using reverse guidance techniques. This enables precise beam control, with the microwave beam accurately directed toward the receiving antenna. JAXA conducted research and development on efficient directional control technology, successfully transmitting 340 W of microwave power to a receiver 55 m away. This marked the first completion of a high-precision directional power experiment, as shown in Figure 19D.²⁴¹ Furthermore, Texas A&M University conducted an M-WPT experiment on the island of Hawaii, with a transmission array antenna shown in Figure 19E.²⁴² They achieved a transmission distance of 148 km, the farthest in the field of M-WPT transmission to date. However, the experiment's transmission efficiency was very low due to the small size of the transmitting and receiving arrays. The effective operation of M-WPT requires a balance between transmission efficiency, transmission distance, and device size. Therefore, before attempting another comprehensive M-WPT test, focusing on improving specific subsystems such as optimizing solar panels' efficiency may be meaningful.²⁴²

L-WPT technology, using laser beams for energy carriage, is suitable for long-distance drone power supply, emergency space station power, and interconnecting spacecraft power supply. NASA's L-WPT flight experiments with micro aerial vehicles have successfully provided 6 W of power, supporting over 15 min of continuous flight.¹³⁶ Laser-Motive company's extensive L-WPT research includes experiments on laser-driven space elevators and drones. Their indoor tests increased drone endurance by 24 times, and the laser power reached 1 kW over 1 km, with overall system efficiency exceeding 10%.²⁴³ Experiments on spacecraft L-WPT application achieved a laser wavelength of 810 nm, 28-W laser power, a maximum 200-m transmission distance, and about 15% overall system efficiency.⁵¹ The US Naval Research Laboratory (NRL) successfully conducted L-WPT over 325 m between two 13-foot-high

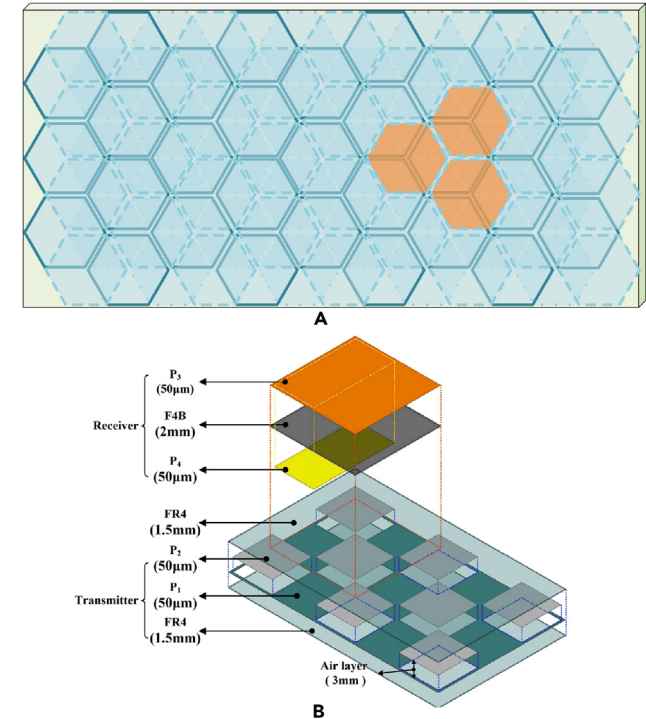
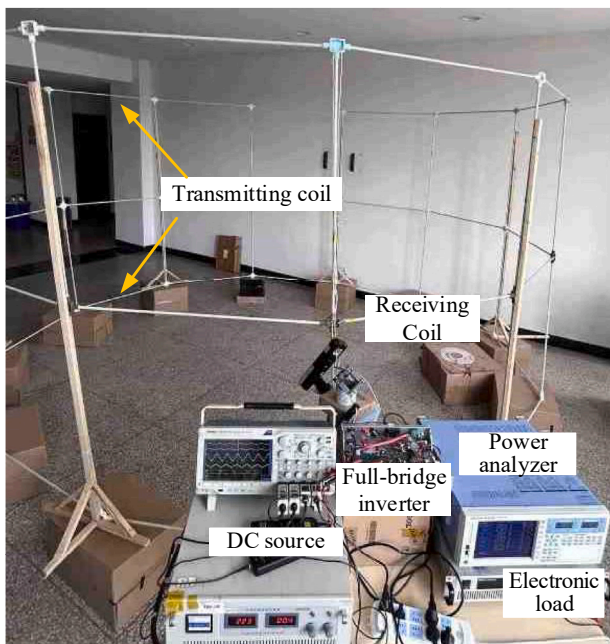


Figure 15. Free-positioning method
(A) Multiple overlapping coils. (B) Capacitive coupler array.



A



B

Figure 16. Large-scale free space WPT

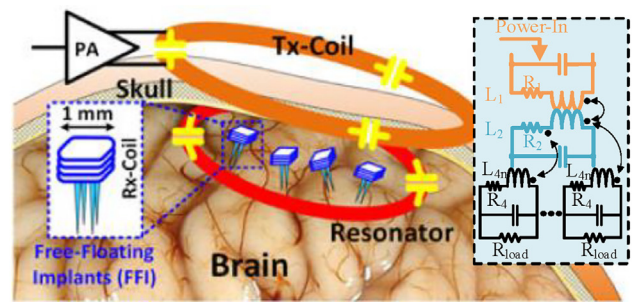
(A) The room-scale WPT system is based on the termed multi-mode quasi-static cavity resonance method (18 m³). (B) Large-space WPT system prototype (25 m³).

towers, as shown in Figure 19F.¹⁷⁵ Current L-WPT technology research is exploratory, focusing on device performance enhancement.

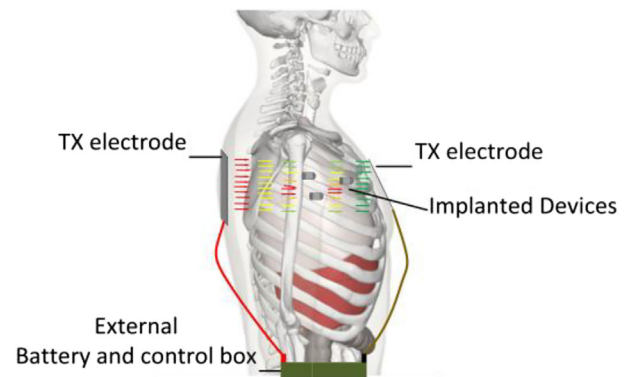
In challenging environments like under water, oilfield drilling, UAVs, and aerospace, WPT faces unique challenges such as seawater's electrical conductivity, extreme physical conditions, and efficient long-distance power transfer. Advancing materials, engineering approaches, and system designs are crucial for overcoming these obstacles and realizing WPT's potential in special industrial applications.

Cost

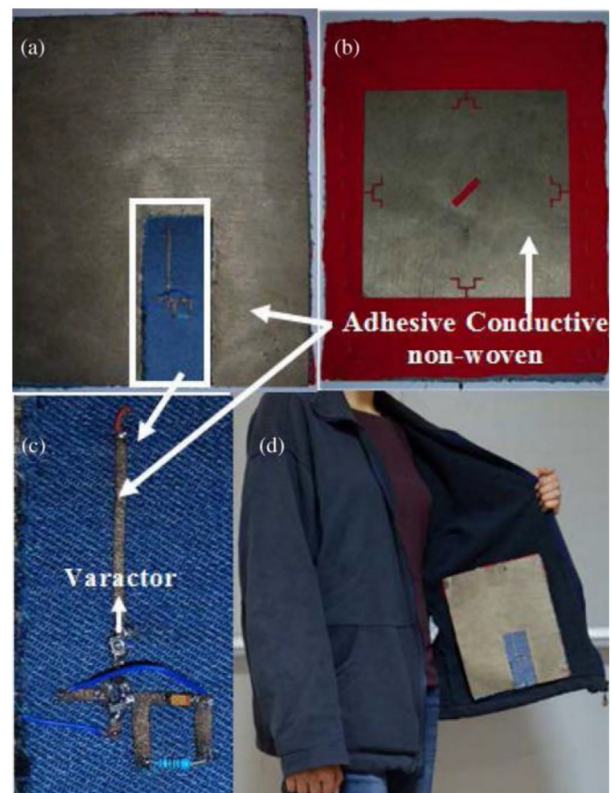
In practical applications, the cost and benefits of the system are unavoidable issues, and the assessment of initial construction costs and subsequent maintenance expenses is a prerequisite for determining the feasibility of the project. Currently, WPT technology has been successfully commercialized in consumer products (such as watches and mobile phones) and SCEVs, bringing convenience but



A



B



C

Figure 17. The application of WPT in IMDs

(A) Conceptual rendering of the WPT link for distributed free-floating implants encompassed by an implanted high-Q resonator and simplified equivalent circuit. (B) Practical system representation with EC-WPT technology. (C) Photographs of the wearable rectenna devices.

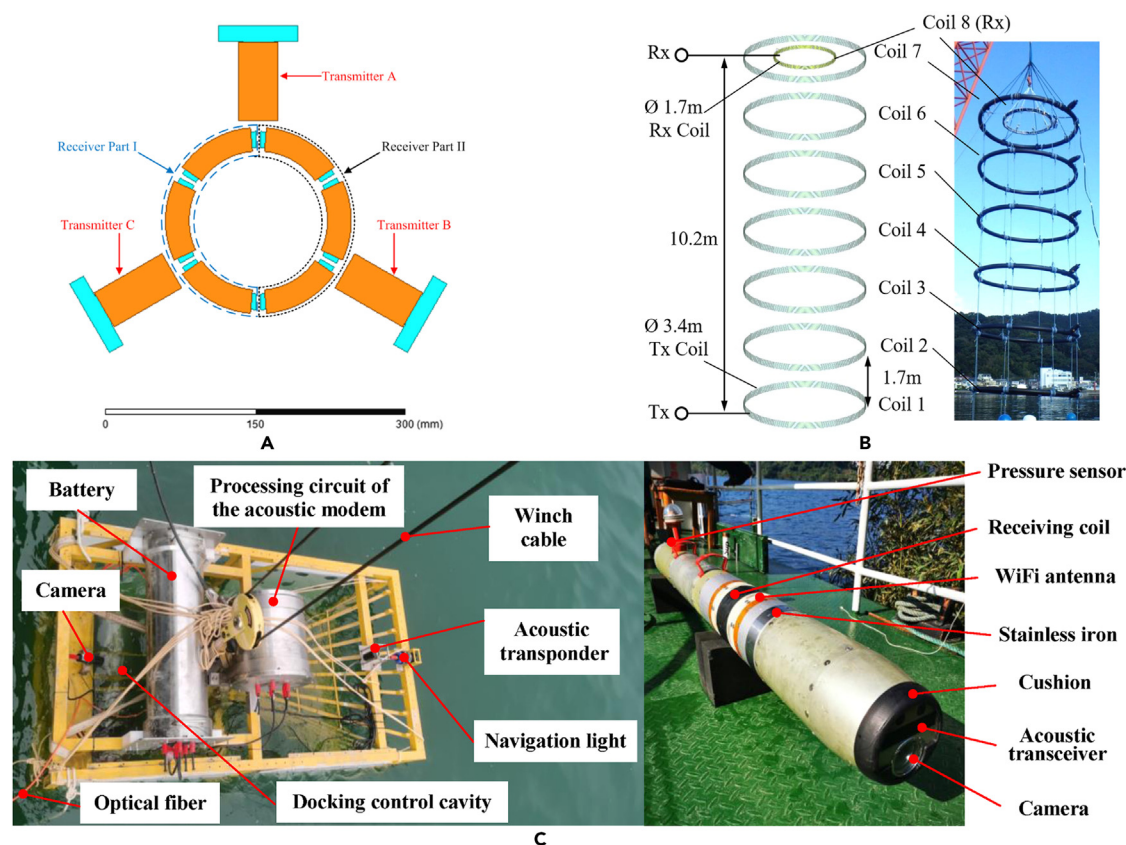


Figure 18. Underwater application

(A) Rotation-resilient structure for underwater WPT system. (B) Circuit construction of WPT system with multiple coils and scene of experiments. (C) Configuration of the docking station and UUV.

also increasing equipment and charging costs.^{8,11} The cost mainly comes from magnetic coupling structures and additional conversion components. Additionally, considering safety factors, it is challenging for its efficiency and power levels to compete with wired charging systems. Large-scale commercialization still requires the iteration of wide-bandgap devices and a corresponding decrease in component costs. For some special applications, the convenience and benefits brought by WPT technology far outweigh the construction costs. For example, in IMDs, UWPT, and SSPS.^{2,7,244} However, WPT technology is still in the exploration and research stage for these applications, with a significant gap from commercialization. The specific research status of application has been reviewed and will not be reiterated here. Therefore, this section mainly discusses the cost and subsequent fees related to the RPEV projects, which have received significant attention.

For the practical engineering of RPEVs, the main costs come from equipment initial investment, construction costs, later maintenance, and electricity fees.²⁴⁵ Equipment costs include materials, converters, power supplies, and asphalt costs for road installation. Construction costs depend on labor and mechanical costs, while maintenance costs come from manpower and material costs due to equipment damage. Electricity fees are closely related to local policy support and the construction of basic power infrastructure. Clearly, estimating the costs of RPEVs requires considering multiple factors, which is also an inevitable challenge in the commercialization process. Of course, RPEVs also bring benefits in other aspects. One advantage is the ability to charge through embedded charging infrastructure under roads, allowing the use of smaller and lighter batteries.²⁴⁶ For RPEVs, power track allocation and battery size are key design variables determining system performance. Taking the RPEVs project in Gumi City, South Korea, as an example, a mathematical optimization model was established to quantitatively analyze the benefits of dynamic charging through an eco-

nomic model of battery size and charging infrastructure configuration.²⁴⁷ The total cost of RPEVs will be reduced by 20.8% compared with SCEVs when 18 buses operate for 10 years, despite the need for more initial investment. This is achieved through smaller batteries with longer lifespans, leading to more cost savings. However, since current RPEV projects for commercial applications mainly focus on system reliability rather than economic value, further optimizing the RPEVs system design can further reduce operating costs. In addition, factors such as integrating renewable energy and local power support investments are essential in shortening the RPEV investment payback period. By optimizing strategies for charging prices and electricity procurement, the investment payback period of RPEVs can be shortened by 25%. Even under current optimization policies and strict grid impact restrictions, when RPEVs' efficiency improves to 90% and costs decrease by 50%, the investment payback period can be reduced by 19% and 22%, respectively.²⁴⁸ The promotion of RPEVs also helps reduce local carbon emissions and related externalities. Assuming integration of RPEV systems into highway infrastructure and supporting their use for private travel, analysis of six European countries shows that cost savings in equipment can fully cover RPEV investments. From the perspective of public expenditure, RPEV integration is self-sustainable.²⁴⁹

As for the current MC-WPT technology, the construction cost of RPEVs is roughly between \$1.8 million and \$5.6 million per mile. However, adopting EC-WPT technology can significantly reduce this expenditure. Assuming a cost of \$200,000 per mile, deploying such a system on a single lane (two-way) of the 4.17 million miles of the US highway network will save \$2.76 trillion in battery costs. With a system lifespan of 30 years, an estimated net savings of about \$6.5 trillion can be achieved. This would be very attractive, and it does not include the cost of millions of wired fast chargers and the cost benefits from a more balanced grid.²⁶

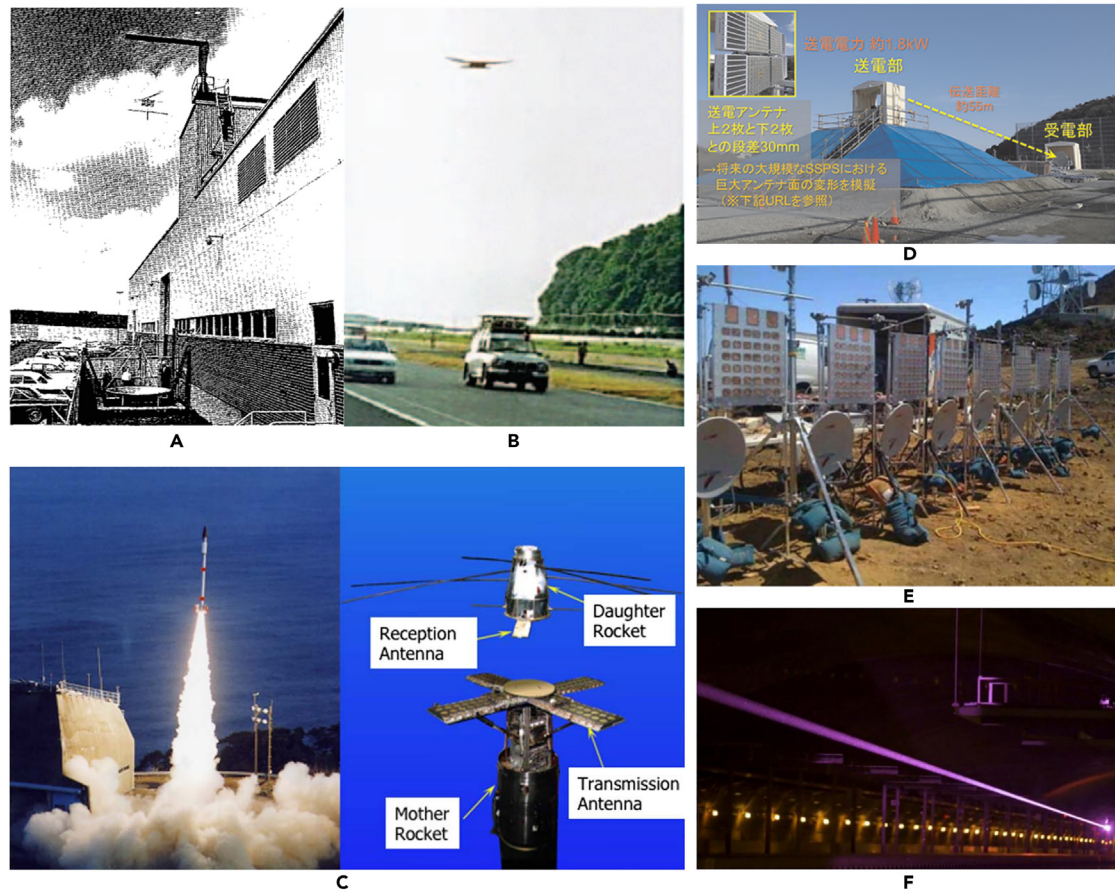


Figure 19. Application with M-WPT and L-WPT technology

(A) M-WPT powers a small helicopter for the first time. (B) The MILAX project in Japan. (C) M-WPT experiment in space. (D) The M-WPT project conducted by JAXA. (E) Managed Energy Technologies, Texas A&M University, University of Kobe 2008 Hawaii M-WPT experiment. (F) L-WPT demonstration in Maryland, USA, on May 23, 2019.

Undoubtedly, as the number of EVs continues to increase, RPEVs are becoming a feasible solution for future transportation. They can not only reduce the infrastructure costs of commercialization but also improve the interoperability of EVs. However, reducing costs requires further research on WPT technology, such as improving efficiency and power levels, researching segmented switching technology, etc.⁹

DISCUSSION

After nearly 2 decades of rapid development, WPT technology already has a certain degree of practicality, and the MC-WPT technology has received the most attention from researchers due to its balanced performance. Mature products have emerged in various industrial applications. However, there are still some problems that need further research and resolution, including safety concerns, large-scale free space WPT technology, simultaneous wireless power and data transfer (SWPDT), and so on.

Electromagnetic environmental safety

Ensuring electromagnetic environmental safety is paramount in the adoption of WPT technology, encompassing EMF management, EMI suppression, and compliance with electromagnetic safety standards. Magnetic coupling WPT systems necessitate adherence to international guidelines, such as ICNIRP2020 and regulations by the Federal Communications Commission and IEEE, to protect against EMF exposure risks.²⁵⁰⁻²⁵² For high-power WPT applications, including EV charging, standards like SAE J2954 specify safety design requirements. In applications involving prolonged human exposure, such as in smart

homes and medical devices, designs must minimize EMF impacts without sacrificing efficiency.²⁵² EMC becomes critical as device connectivity and power levels increase, requiring effective EMI suppression through optimized system design, electromagnetic shielding, and the use of advanced materials like nanocrystalline cores and metamaterials. In the future, attention should be paid to electromagnetic shielding technologies for special applications like IMDs, underwater WPT, and drilling, as well as fully utilizing the performance of electromagnetic shielding materials.

Large-scale free space WPT

WPT technology, particularly MC-WPT, is crucial for charging consumer electronics within a limited range, suitable for stationary applications but less effective for mobile device charging in larger spaces. Recent advancements have expanded WPT's reach to cover areas of 18 m³ and 25 m³,^{214,215} showcasing the potential for convenient charging across extensive spaces. However, challenges in boosting power transmission and efficiency, alongside ensuring human safety, hinder broader deployment. Key hurdles include extending transmission distances and improving efficiency without compromising safety or economic viability. Innovative solutions, such as employing metamaterials and refining electromagnetic designs, are under exploration to enhance resonant structures and energy capture methods. Addressing energy management in large-scale applications demands smarter systems with integrated sensors and real-time adjustments for efficient and safe energy distribution. The evolution of large-scale WPT opens new avenues for mobile charging and wireless energy networks, promising significant advancements and commercial opportunities shortly.

Simultaneous wireless power and data transfer

SWPDT has advanced significantly, with various systems offering unique benefits for different applications. Despite progress, challenges like energy conversion efficiency, signal interference, and system complexity persist.^{224,253,254} Current technologies primarily support point-to-point communication, with high-frequency transmissions facing issues of signal interference. Future SWPDT research must focus on enhancing efficiency and signal transmission rates and developing efficient energy converters and modulation techniques. The technology's potential in IoT, smart homes, and health monitoring underscores the need for multi-node communication capabilities. For widespread adoption, establishing comprehensive policies and standards for safety, interoperability, and environmental impact is crucial, addressing technical and commercialization challenges.

Efficiency improvement in far-field WPT

Far-field technology holds the potential to enable WPT over considerable distances, making it particularly relevant for applications such as powering or charging devices in remote locations, IoT devices, and consumer electronics that lack a direct line of sight. However, this technology faces significant challenges, including lower power efficiency over longer distances, regulatory and safety concerns regarding the transmission of high-power beams, and the necessity for precise beam targeting and alignment to ensure efficient energy transfer. Improving the efficiency of any far-field WPT system poses a formidable task. As advancements in far-field WPT systems continue to expand, so do their potential applications. However, the overall efficiency remains unsuitable for commercial development, with M-WPT and L-WPT systems achieving only around 50% and 20% efficiency, respectively, presenting a major obstacle. The research community is concentrating on enhancing efficiency for commercial deployment, with researchers striving to improve PV cell efficiency.

CONCLUSION

This paper provides a comprehensive review of the latest research, challenges, and broad application prospects of WPT technology. It delves into various WPT methods, including near-field and far-field technologies, electromagnetic coupling, electric field coupling, microwaves, and lasers. The review details the fundamental working principles, strategies for performance enhancement, and practical applications of various WPT technologies. Additionally, the paper also addresses practical application challenges such as safety considerations and electromagnetic interference.

The paper begins with an examination of the basic principles of four typical WPT technologies, comparing and analyzing their respective strengths and weaknesses. It then focuses on the research priorities of each technology and presents advanced techniques for enhancing performance and addressing current challenges. The review particularly highlights the impact of new physical concepts and novel materials in advancing WPT technology. The potential of metamaterials and metasurfaces as a promising avenue for future technological advancements is also explored. Special emphasis is placed on the standardization and practical implementation of WPT across various domains, including EVs, medical implant devices, underwater environments, and aerospace.

The paper concludes by identifying new research directions and unresolved issues, including safety concerns, large-space WPT, and SWPDT. This comprehensive review is intended to foster a deeper understanding of WPT systems and their diverse applications in modern technology. Despite current challenges and limitations, WPT technology is anticipated to play an increasingly vital role in a wider array of applications, driving innovation and progress in energy transmission methods.

AUTHOR CONTRIBUTIONS

Conceptualization, Z.L. and S.L.; investigation, Z.L., C.M., and S.L.; writing – original draft, Z.L. and T.L.; writing – review & editing, Z.L., C.M., and S.L.; funding acquisition, C.M. and S.L.; resources, C.M. and S.L.; supervision, C.M. and S.L.

DECLARATION OF INTERESTS

The authors declare no competing interests.

REFERENCES

1. Tesla, N., and White, W. (1999). High frequency oscillators for electro-therapeutic and other purposes. *Proc. IEEE* 87, 1282.
2. Glaser, P.E. (1968). Power from the sun: Its future. *Science* 162, 857-861.
3. Rim, C.T., and Mi, C. (2017). *Wireless Power Transfer for Electric Vehicles and Mobile Devices* (John Wiley & Sons).
4. Roy, S., Azad, A.N.M.W., Baidya, S., et al. (2022). Powering solutions for biomedical sensors and implants inside the human body: a comprehensive review on energy harvesting units, energy storage, and wireless power transfer techniques. *IEEE Trans. Power Electron.* 37, 12237-12263.
5. Siqi, L., and Mi, C.C. (2015). Wireless Power Transfer for Electric Vehicle Applications. *IEEE J. Sel. Topics Pow. Electron.* 3, 4-17.
6. Bi, Z., Song, L., De Kleine, R., et al. (2015). Plug-in vs. wireless charging: Life cycle energy and greenhouse gas emissions for an electric bus system. *Appl. Energy* 146, 11-19.
7. Moore, J., Castellanos, S., Xu, S., et al. (2019). Applications of wireless power transfer in medicine: State-of-the-art reviews. *Ann. Biomed. Eng.* 47, 22-38.
8. Fareq, M., Fitra, M., Irwanto, M., et al. (2014). Low wireless power transfer using inductive coupling for mobile phone charger. In *Paper Presented at: Journal of Physics: Conference Series* (IOP Publishing).
9. Mi, C.C., Buja, G., Choi, S.Y., et al. (2016). Modern Advances in Wireless Power Transfer Systems for Roadway Powered Electric Vehicles. *IEEE Trans. Ind. Electron.* 63, 6533-6545.
10. Assaworarith, S., Yu, X., and Fan, S. (2017). Robust wireless power transfer using a nonlinear parity-time-symmetric circuit. *Nature* 546, 387-390.
11. Li, S., Lu, S., and Mi, C.C. (2021). Revolution of electric vehicle charging technologies accelerated by wide bandgap devices. *Proc. IEEE* 109, 985-1003.
12. Gao, M., Yao, Y., Yang, F., et al. (2023). Two-dimensional materials for wireless power transfer. *Device* 1, 100022.
13. Bi, Z., Kan, T., Mi, C.C., et al. (2016). A review of wireless power transfer for electric vehicles: Prospects to enhance sustainable mobility. *Appl. Energy* 179, 413-425.
14. Covic, G.A., and Boys, J.T. (2013). Inductive power transfer. *Proc. IEEE* 101, 1276-1289.
15. Dai, J., and Ludois, D.C. (2015). A survey of wireless power transfer and a critical comparison of inductive and capacitive coupling for small gap applications. *IEEE Trans. Power Electron.* 30, 6017-6029.
16. Clerckx, B., Kim, J., Choi, K.W., et al. (2022). Foundations of wireless information and power transfer: Theory, prototypes, and experiments. *Proc. IEEE* 110, 8-30.
17. Mohsan, S.A.H., Qian, H., and Amjad, H. (2023). A comprehensive review of optical wireless power transfer technology. *Front Inform Tech EI* 24, 767-800.
18. Zhang, Z., Pang, H., Georgiadis, A., et al. (2019). Wireless power transfer—An overview. *IEEE Trans. Ind. Electron.* 66, 1044-1058.
19. Birajdar, S.R. (1981). WIRELESS ENERGY TRANSMISSION. *Trans Microw Theory Techn* 29, 1319-1327.
20. Zhang, W., and Mi, C.C. (2016). Compensation topologies of high-power wireless power transfer systems. *IEEE Trans. Veh. Technol.* 65, 4768-4778.
21. Li, S., and Mi, C.C. (2014). Wireless power transfer for electric vehicle applications. *IEEE J. Sel. Topics Pow Electron* 3, 4-17.
22. Kurs, A., Karalis, A., Moffatt, R., et al. (2007). Wireless power transfer via strongly coupled magnetic resonances. *Science* 317, 83-86.
23. Van Schuylenbergh, K., and Puers, R. (2009). *Inductive Powering: Basic Theory and Application to Biomedical Systems* (Springer).
24. Hou, X., Hu, H., Su, Y., et al. (2023). A Multirelay Wireless Power Transfer System With Double-Sided LCC Compensation Network for Online Monitoring Equipment. *IEEE J. Sel. Topics Pow Electron* 11, 1262-1271.
25. Liu, C. (2011). *Fundamental Study on Capacitively Coupled Contactless Power Transfer Technology* (ResearchSpace@ Auckland).

26. Afridi, K. (2022). The future of electric vehicle charging infrastructure. *Nat. Electron.* 5, 62-64.
27. Li, S., Liu, Z., Zhao, H., et al. (2016). Wireless power transfer by electric field resonance and its application in dynamic charging. *IEEE Trans. Ind. Electron.* 63, 6602-6612.
28. Luo, B., Hu, A.P., Munir, H., et al. (2022). Compensation network design of CPT systems for achieving maximum power transfer under coupling voltage constraints. *IEEE J. Sel. Topics Pow Electron* 10, 138-148.
29. Lu, F., Zhang, H., and Mi, C. (2017). A review on the recent development of capacitive wireless power transfer technology. *Energies* 10, 1752.
30. Zhang, H., Lu, F., Hofmann, H., et al. (2016). A four-plate compact capacitive coupler design and LCL-compensated topology for capacitive power transfer in electric vehicle charging application. *IEEE Trans. Power Electron.* 31, 8541-8551.
31. Liu, Z., Su, Y., Hu, H., et al. (2023). Research on transfer mechanism and power improvement technology of the SCC-WPT system. *IEEE Trans. Power Electron.* 38, 1324-1335.
32. Zou, L.J., Zhu, Q., Van Neste, C.W., et al. (2021). Modeling single-wire capacitive power transfer system with strong coupling to ground. *IEEE J. Sel. Topics Power Electron.* 9, 2295-2302.
33. Lu, F., Zhang, H., and Mi, C. (2018). A two-plate capacitive wireless power transfer system for electric vehicle charging applications. *IEEE Trans. Power Electron.* 33, 964-969.
34. Liu, Z., Hu, H., Su, Y., et al. (2023). A Double-Receiver Compact SCC-WPT System with CV/CC Output for Mobile Devices Charging/Supply. *IEEE Trans. Power Electron.* 38, 9230-9245.
35. Sinha, S., Kumar, A., Regensburger, B., et al. (2019). A new design approach to mitigating the effect of parasitics in capacitive wireless power transfer systems for electric vehicle charging. *IEEE Trans. Transp. Electrification.* 5, 1040-1059.
36. Pries, J., Galigekere, V.P.N., Onar, O.C., et al. (2020). A 50-kW three-phase wireless power transfer system using bipolar windings and series resonant networks for rotating magnetic fields. *IEEE Trans. Power Electron.* 35, 4500-4517.
37. Mihret, F., Srinivas, T., Hegde, G., et al. (2022). Integrated photonics for RF/microwave analog signal processing of wireless systems: a review article. *ISSS J. Micro. Smart Sys.* 11, 235-256.
38. Soltani, M.D., Sarbazi, E., Bamiedakis, N., et al. (2022). Safety analysis for laser-based optical wireless communications: A tutorial. *Proc. IEEE* 8, 1045-1072.
39. Zhu, X., Jin, K., Hui, Q., et al. (2021). Long-range wireless microwave power transmission: A review of recent progress. *IEEE J. Sel. Topics Power Electron.* 9, 4932-4946.
40. Jin, K., and Zhou, W. (2019). Wireless laser power transmission: A review of recent progress. *IEEE Trans. Power Electron.* 34, 3842-3859.
41. Carvalho, N.B., Georgiadis, A., Costanzo, A., et al. (2014). Wireless power transmission: R&D activities within Europe. *IEEE Trans Microw Theory Techn* 62, 1031-1045.
42. McSpadden, J.O., and Mankins, J.C. (2002). Space solar power programs and microwave wireless power transmission technology. *IEEE Microw. Mag.* 3, 46-57.
43. Tsai, W.-S., Lu, H.-H., Wu, H.-W., et al. (2019). A 30 Gb/s PAM4 underwater wireless laser transmission system with optical beam reducer/expander. *Sci. Rep.* 9, 8605.
44. Zhu, X., Jin, K., and Hui, Q. (2021). Near-field power-focused directional radiation in microwave wireless power transfer system. *IEEE J. Sel. Topics Power Electron.* 9, 1147-1156.
45. Tran, L.-G., Cha, H.-K., and Park, W.-T. (2017). RF power harvesting: a review on designing methodologies and applications. *Micro Nano Sys. Lett.* 5, 14.
46. Ullah, M.A., Keshavarz, R., Abolhasan, M., et al. (2022). A review on antenna technologies for ambient rf energy harvesting and wireless power transfer: Designs, challenges and applications. *IEEE Access* 10, 17231-17267.
47. Clerckx, B., and Bayguzina, E. (2016). Waveform design for wireless power transfer. *IEEE Trans. Signal Process.* 64, 6313-6328.
48. Degenford, J.E., Sirkis, M., and Steier, W. (1964). The reflecting beam waveguide. *IEEE Trans. Microw. Theor. Tech.* 12, 445-453.
49. Soares Boaventura, A.J., Collado, A., Georgiadis, A., et al. (2014). Spatial power combining of multi-sine signals for wireless power transmission applications. *IEEE Trans. Microw. Theor. Tech.* 62, 1022-1030.
50. Lin, M., and Zhong, W. (2023). Design principles and implementation of receiver positioning and beam steering for laser power transfer systems. *iScience* 26, 108182.
51. Shi, D., Zhang, L., Ma, H., et al. (2016). Research on wireless power transmission system between satellites. In Paper Presented at: 2016 IEEE Wireless Power Transfer Conference (WPTC) (IEEE).
52. Liu, Q., Wu, J., Xia, P., et al. (2016). Charging unplugged: Will distributed laser charging for mobile wireless power transfer work? *IEEE Veh. Technol. Mag.* 11, 36-45.
53. He, T., Zhang, L., Zheng, G., et al. (2021). Analysis and experiment of the laser wireless energy transmission efficiency based on the receiver of powersphere. *IEEE Access* 9, 55340-55351.
54. Zhou, W., and Jin, K. (2015). Efficiency evaluation of laser diode in different driving modes for wireless power transmission. *IEEE Trans. Power Electron.* 30, 6237-6244.
55. Ahmed, J., and Salam, Z. (2015). An improved method to predict the position of maximum power point during partial shading for PV arrays. *IEEE Trans. Ind. Inf.* 11, 1378-1387.
56. Mason, R. (2011). Feasibility of Laser Power Transmission to a High-Altitude Unmanned Aerial Vehicle (RAND).
57. Costanzo, A., and Masotti, D. (2017). Energizing 5G: Near-and far-field wireless energy and data transfer as an enabling technology for the 5G IoT. *IEEE Microw. Mag.* 18, 125-136.
58. Costanzo, A., Dionigi, M., Masotti, D., et al. (2014). Electromagnetic energy harvesting and wireless power transmission: A unified approach. *Proc. IEEE* 102, 1692-1711.
59. Raible, D.E. (2011). Free Space Optical Communications with High Intensity Laser Power Beaming (Cleveland State University).
60. Erickson, R.W., and Maksimovic, D. (2007). *Fundamentals of Power Electronics* (Springer Science & Business Media).
61. Wang, C.-S., Covic, G.A., and Stielau, O.H. (2004). Investigating an LCL load resonant inverter for inductive power transfer applications. *IEEE Trans. Power Electron.* 19, 995-1002.
62. Keeling, N.A., Covic, G.A., and Boys, J.T. (2010). A unity-power-factor IPT pickup for high-power applications. *IEEE Trans. Ind. Electron.* 57, 744-751.
63. Auvigne, C., Germano, P., Ladas, D., et al. (2012). A dual-topology ICPT applied to an electric vehicle battery charger. In Paper Presented at: 2012 XXth International Conference on Electrical Machines (IEEE).
64. Wang, C.-S., Stielau, O.H., and Covic, G.A. (2005). Design considerations for a contactless electric vehicle battery charger. *IEEE Trans. Ind. Electron.* 52, 1308-1314.
65. Pantic, Z., Bai, S., and Lukic, S.M. (2011). ZCS π LCC π -compensated resonant inverter for inductive-power-transfer application. *IEEE Trans. Ind. Electron.* 58, 3500-3510.
66. Li, S., Li, W., Deng, J., et al. (2015). A double-sided LCC compensation network and its tuning method for wireless power transfer. *IEEE Trans. Veh. Technol.* 64, 2261-2273.
67. Lu, J., Zhu, G., Lin, D., et al. (2019). Unified load-independent ZPA analysis and design in CC and CV modes of higher order resonant circuits for WPT systems. *IEEE Trans. Transp. Electrification.* 5, 977-987.
68. Zhang, Y., Kan, T., Yan, Z., et al. (2019). Modeling and analysis of series- π compensation for wireless power transfer systems with a strong coupling. *IEEE Trans. Power Electron.* 34, 1209-1215.
69. Zhao, L., Thrimawithana, D.J., and Madawala, U.K. (2017). Hybrid bidirectional wireless EV charging system tolerant to pad misalignment. *IEEE Trans. Ind. Electron.* 64, 7079-7086.
70. Zhao, L., Thrimawithana, D.J., Madawala, U.K., et al. (2019). A misalignment-tolerant series-hybrid wireless EV charging system with integrated magnetics. *IEEE Trans. Power Electron.* 34, 1276-1285.

71. Mai, R., Yang, B., Chen, Y., et al. (2019). A misalignment tolerant IPT system with intermediate coils for constant-current output. *IEEE Trans. Power Electron.* 34, 7151-7155.
72. Choi, S.Y., Huh, J., Lee, W.Y., et al. (2014). Asymmetric coil sets for wireless stationary EV chargers with large lateral tolerance by dominant field analysis. *IEEE Trans. Power Electron.* 29, 6406-6420.
73. Yao, Y., Wang, Y., Liu, X., et al. (2019). A novel unsymmetrical coupling structure based on concentrated magnetic flux for high-misalignment IPT applications. *IEEE Trans. Power Electron.* 34, 3110-3123.
74. Aditya, K., Sood, V.K., and Williamson, S.S. (2017). Magnetic characterization of unsymmetrical coil pairs using Archimedean spirals for wider misalignment tolerance in IPT systems. *IEEE Trans. Transp. Electrification.* 3, 454-463.
75. Budhia, M., Boys, J.T., Covic, G.A., et al. (2013). Development of a single-sided flux magnetic coupler for electric vehicle IPT charging systems. *IEEE Trans. Ind. Electron.* 60, 318-328.
76. Zaheer, A., Covic, G.A., and Kacprzak, D. (2014). A bipolar pad in a 10-kHz 300-W distributed IPT system for AGV applications. *IEEE Trans. Ind. Electron.* 61, 3288-3301.
77. Li, S., Yu, X., Yuan, Y., et al. (2023). A Novel High-Voltage Power Supply with MHz WPT Techniques: Achieving High-Efficiency, High-Isolation, and High-Power-Density. *IEEE Trans. Power Electron.* 38, 14794-14805.
78. Zhang, Z., and Chau, K.T. (2015). Homogeneous wireless power transfer for move-and-charge. *IEEE Trans. Power Electron.* 30, 6213-6220.
79. Lin, D., Zhang, C., and Hui, S.Y.R. (2017). Mathematic analysis of omnidirectional wireless power transfer—Part-II three-dimensional systems. *IEEE Trans. Power Electron.* 32, 613-624.
80. Feng, T., Sun, Y., Zuo, Z., et al. (2022). Magnetic field analysis and excitation currents optimization for an omnidirectional WPT system based on three-phase tubular coils. *IEEE Trans. Ind. Appl.* 58, 1268-1278.
81. Liu, G., Zhang, B., Xiao, W., et al. (2018). Omnidirectional wireless power transfer system based on rotary transmitting coil for household appliances. *Energies* 11, 878.
82. Feng, T., Zuo, Z., Sun, Y., et al. (2022). A reticulated planar transmitter using a three-dimensional rotating magnetic field for free-positioning omnidirectional wireless power transfer. *IEEE Trans. Power Electron.* 37, 9999-10015.
83. Deng, Q., Liu, J., Czarkowski, D., et al. (2017). An inductive power transfer system supplied by a multiphase parallel inverter. *IEEE Trans. Ind. Electron.* 64, 7039-7048.
84. Hao, H., Covic, G.A., and Boys, J.T. (2013). A parallel topology for inductive power transfer power supplies. *IEEE Trans. Power Electron.* 29, 1140-1151.
85. Wang, C.-S., Covic, G.A., and Stielau, O.H. (2004). Power transfer capability and bifurcation phenomena of loosely coupled inductive power transfer systems. *IEEE Trans. Ind. Electron.* 51, 148-157.
86. Borage, M., Tiwari, S., and Kotaiah, S. (2005). Analysis and design of an LCL-T resonant converter as a constant-current power supply. *IEEE Trans. Ind. Electron.* 52, 1547-1554.
87. Huh, J., Lee, S.W., Lee, W.Y., et al. (2011). Narrow-width inductive power transfer system for online electrical vehicles. *IEEE Trans. Power Electron.* 26, 3666-3679.
88. Sharp, B., and Wu, H. (2012). Asymmetrical voltage-cancellation control for LCL resonant converters in inductive power transfer systems. In Paper Presented at: 2012 Twenty-Seventh Annual IEEE Applied Power Electronics Conference and Exposition (APEC) (IEEE).
89. Berger, A., Agostinelli, M., Vesti, S., et al. (2015). A wireless charging system applying phase-shift and amplitude control to maximize efficiency and extractable power. *IEEE Trans. Power Electron.* 30, 6338-6348.
90. Yeo, T.-D., Kwon, D., Khang, S.-T., et al. (2017). Design of maximum efficiency tracking control scheme for closed-loop wireless power charging system employing series resonant tank. *IEEE Trans. Power Electron.* 32, 471-478.
91. Tang, X., Zeng, J., Pun, K.P., et al. (2018). Low-cost maximum efficiency tracking method for wireless power transfer systems. *IEEE Trans. Power Electron.* 33, 5317-5329.
92. Liu, C., Hu, A.P., Covic, G.A., et al. (2011). Comparative study of CCPT systems with two different inductor tuning positions. *IEEE Trans. Power Electron.* 27, 294-306.
93. Jegadeesan, R., Agarwal, K., Guo, Y.-X., et al. (2017). Wireless power delivery to flexible subcutaneous implants using capacitive coupling. *IEEE Trans. Microw. Theor. Tech.* 65, 280-292.
94. Ludois, D.C., Reed, J.K., and Hanson, K. (2012). Capacitive power transfer for rotor field current in synchronous machines. *IEEE Trans. Power Electron.* 27, 4638-4645.
95. Ludois, D.C., Erickson, M.J., and Reed, J.K. (2014). Aerodynamic fluid bearings for translational and rotating capacitors in noncontact capacitive power transfer systems. *IEEE Trans. Ind. Appl.* 50, 1025-1033.
96. Lu, F., Zhang, H., Hofmann, H., et al. (2015). A Double-Sided *LCLC*-Compensated Capacitive Power Transfer System for Electric Vehicle Charging. *IEEE Trans. Power Electron.* 30, 6011-6014.
97. Sohn, Y.H., Choi, B.H., Lee, E.S., et al. (2015). General unified analyses of two-capacitor inductive power transfer systems: Equivalence of current-source SS and SP compensations. *IEEE Trans. Power Electron.* 30, 6030-6045.
98. Wang, Y., Zhang, H., and Lu, F. (2022). Review, analysis, and design of four basic CPT topologies and the application of high-order compensation networks. *IEEE Trans. Power Electron.* 37, 6181-6193.
99. Huang, L., Hu, A.P., Swain, A.K., et al. (2016). Z-impedance compensation for wireless power transfer based on electric field. *IEEE Trans. Power Electron.* 31, 7556-7563.
100. Su, Y.-G., Zhao, Y.-M., Hu, A.P., et al. (2019). An F-type compensated capacitive power transfer system allowing for sudden change of pickup. *IEEE J. Sel. Topics Power Electron.* 7, 1084-1093.
101. Liu, Z., Su, Y.-G., Zhao, Y.-M., et al. (2021). Capacitive power transfer system with double T-type resonant network for mobile devices charging/supply. *IEEE Trans. Power Electron.* 37, 2394-2403.
102. Vu, V.-B., Dahidah, M., Pickert, V., et al. (2020). An improved LCL-L compensation topology for capacitive power transfer in electric vehicle charging. *IEEE Access* 8, 27757-27768.
103. Kusunoki, M., Obara, D., and Masuda, M. (2014). Wireless power transfer via electric field resonance coupling. In Paper Presented at: 2014 Asia-Pacific Microwave Conference (APMC).
104. Lu, F., Zhang, H., Hofmann, H., et al. (2018). A double-sided LC-compensation circuit for loosely coupled capacitive power transfer. *IEEE Trans. Power Electron.* 33, 1633-1643.
105. Liu, Y., Wu, T., and Fu, M. (2021). Interleaved capacitive coupler for wireless power transfer. *IEEE Trans. Power Electron.* 36, 13526-13535.
106. Xia, J., Yuan, X., Lu, S., et al. (2022). A two-stage parameter optimization method for capacitive power transfer systems. *IEEE Trans. Power Electron.* 37, 1102-1117.
107. Hagen, S., Tisler, M., Dai, J., et al. (2022). Use of the rotating rectifier board as a capacitive power coupler for brushless wound field synchronous machines. *IEEE J. Sel. Topics Power Electron.* 10, 170-183.
108. Zhu, J.-Q., Ban, Y.-L., Zhang, Y., et al. (2019). A novel capacitive coupler array with free-positioning feature for mobile tablet applications. *IEEE Trans. Power Electron.* 34, 6014-6019.
109. Yuan, H., Liang, C., Zhang, R., et al. (2023). A novel anti-offset interdigital electrode capacitive coupler for mobile desktop charging. *IEEE Trans. Power Electron.* 38, 4140-4151.
110. Wang, Y., Sun, Z., Guan, Y., et al. (2023). Overview of Megahertz Wireless Power Transfer. *Proc. IEEE* 111, 528-554.
111. Vu, V.-B., Kamal, L.B.M., Tay, J., et al. (2017). A multi-output capacitive charger for electric vehicles. In Paper Presented at: 2017 IEEE 26th International Symposium on Industrial Electronics (ISIE) (IEEE).
112. Liu, C., Hu, A.P., Wang, B., et al. (2013). A capacitively coupled contactless matrix charging platform with soft switched transformer control. *IEEE Trans. Ind. Electron.* 60, 249-260.
113. Abramov, E., and Peretz, M.M. (2020). Multi-loop control for power transfer regulation in capacitive wireless systems by means of variable matching networks. *IEEE J. Sel. Topics Power Electron.* 8, 2095-2110.
114. Qing, X., Su, Y., Hu, A.P., et al. (2022). Dual-Loop Control Method for CPT System Under Coupling Misalignments and Load Variations. *IEEE J. Sel. Topics Power Electron.* 10, 4902-4912.

115. Jaffe, P., and McSpadden, J. (2013). Energy conversion and transmission modules for space solar power. *Proc. IEEE* 101, 1424-1437.
116. Huang, T., Axelsson, O., Bergsten, J., et al. (2020). Impact of AlGaIn/GaN interface and passivation on the robustness of low-noise amplifiers. *IEEE Trans. Electron. Dev.* 67, 2297-2303.
117. Gilasgar, M., Barlabé, A., and Pradell, L. (2020). High-efficiency reconfigurable dual-band class-F power amplifier with harmonic control network using MEMS. *IEEE Microw. Wireless Compon. Lett.* 30, 677-680.
118. Woo, Y.-Y., Yang, Y., and Kim, B. (2006). Analysis and experiments for high-efficiency class-F and inverse class-F power amplifiers. *IEEE Trans. Microw. Theor. Tech.* 54, 1969-1974.
119. Cipriani, E., Colantonio, P., Giannini, F., et al. (2010). Theoretical and experimental comparison of Class F vs. Class F+ 1 PAs. In Paper Presented at: The 5th European Microwave Integrated Circuits Conference (IEEE).
120. Li, Y., and Jandhyala, V. (2012). Design of retrodirective antenna arrays for short-range wireless power transmission. *IEEE Trans. Antenn. Propag.* 60, 206-211.
121. Narita, T., Kimura, T., Anma, K., et al. (2011). Development of high accuracy phase control method for space solar power system. In Paper Presented at: 2011 IEEE MTT-S International Microwave Workshop Series on Innovative Wireless Power Transmission: Technologies, Systems, and Applications (IEEE).
122. Massa, A., Oliveri, G., Viani, F., et al. (2013). Array designs for long-distance wireless power transmission: State-of-the-art and innovative solutions. *Proc. IEEE* 101, 1464-1481.
123. Kaya, N., Iwashita, M., Little, F., et al. (2009). Microwave power beaming test in Hawaii. In Paper Presented at: Proceedings International Astronautical Congress IAC'09.
124. Brown, W.C. (1976). Optimization of the efficiency and other properties of the rectenna element. In Paper Presented at: 1976 IEEE-MTT-S International Microwave Symposium (IEEE).
125. Ladan, S., and Wu, K. (2015). Nonlinear modeling and harmonic recycling of millimeter-wave rectifier circuit. *IEEE Trans. Microw. Theor. Tech.* 63, 937-944.
126. Zhang, X.-Y., Du, Z.-X., and Xue, Q. (2017). High-efficiency broadband rectifier with wide ranges of input power and output load based on branch-line coupler. *IEEE Trans. Circ. Syst. I.* 64, 731-739.
127. Ruiz, M.N., Marante, R., and Garcia, J.A. (2012). A class E synchronous rectifier based on an E-pHEMT device for wireless powering applications. In Paper Presented at: 2012 IEEE/MTT-S International Microwave Symposium Digest (IEEE).
128. Kuhn, V., Lahuec, C., Seguin, F., et al. (2015). A Multi-Band Stacked RF Energy Harvester With RF-to-DC Efficiency Up to 84%. *IEEE Trans. Microw. Theor. Tech.* 63, 1768-1778.
129. Olgun, U., Chen, C.-C., and Volakis, J.L. (2011). Investigation of rectenna array configurations for enhanced RF power harvesting. *IEEE Antenn. Wireless Propag. Lett.* 10, 262-265.
130. Costanzo, A., Masotti, D., Romani, A., et al. (2014). Energy scavenging and storage for RFID systems. In *EUMA HIGH FREQUENCY TECHNOLOGIES SERIES*, pp. 38-75.
131. Strassner, B., and Chang, K. (2003). 5.8-GHz circularly polarized dual-rhombic-loop traveling-wave rectifying antenna for low power-density wireless power transmission applications. *IEEE Trans. Microw. Theor. Tech.* 51, 1548-1553.
132. Shinohara, N., and Matsumoto, H. (1998). Experimental study of large rectenna array for microwave energy transmission. *IEEE Trans. Microw. Theor. Tech.* 46, 261-268.
133. Almoneef, T.S., Sun, H., and Ramahi, O.M. (2016). A 3-D folded dipole antenna array for far-field electromagnetic energy transfer. *IEEE Antenn. Wireless Propag. Lett.* 15, 1406-1409.
134. Crump, P., Wang, J., Patterson, S., et al. (2005). SHEDS funding enables power conversion efficiency up to 85% at high powers from 975-nm broad area diode lasers. In Paper Presented at: Presentation at Stanford Photonics Research Center Annual Symp.
135. Sennaroglu, A. (2017). *Solid-state Lasers and Applications* (CRC Press).
136. Raible, D.E. (2008). *High Intensity Laser Power Beaming for Wireless Power Transmission* (Cleveland State University).
137. Ortobasi, U., and Friedman, H. (2006). Powersphere: A photovoltaic cavity converter for wireless power transmission using high power lasers. In Paper Presented at: 2006 IEEE 4th World Conference on Photovoltaic Energy Conference (IEEE).
138. Becker, D.E., Chiang, R., Keys, C.C., et al. (2010). Photovoltaic-concentrator based power beaming for space elevator application. In Paper Presented at: AIP Conference Proceedings (American Institute of Physics).
139. Patel, H., and Agarwal, V. (2008). Maximum power point tracking scheme for PV systems operating under partially shaded conditions. *IEEE Trans. Ind. Electron.* 55, 1689-1698.
140. Kobayashi, K., Takano, I., and Sawada, Y. (2006). A study of a two stage maximum power point tracking control of a photovoltaic system under partially shaded insolation conditions. *Sol. Energy Mater. Sol. Cell.* 90, 2975-2988.
141. Miyatake, M., Veerachary, M., Toriumi, F., et al. (2011). Maximum power point tracking of multiple photovoltaic arrays: A PSO approach. *IEEE Trans. Aero. Electron. Syst.* 47, 367-380.
142. Bender, C.M., and Boettcher, S. (1998). Real spectra in non-Hermitian Hamiltonians having P T symmetry. *Phys. Rev. Lett.* 80, 5243-5246.
143. Makris, K.G., El-Ganainy, R., Christodoulides, D.N., et al. (2008). Beam dynamics in P T symmetric optical lattices. *Phys. Rev. Lett.* 100, 103904.
144. Guo, A., Salamo, G.J., Duchesne, D., et al. (2009). Observation of P T-symmetry breaking in complex optical potentials. *Phys. Rev. Lett.* 103, 093902.
145. Rüter, C.E., Makris, K.G., El-Ganainy, R., et al. (2010). Observation of parity-time symmetry in optics. *Nat. Phys.* 6, 192-195.
146. Chang, L., Jiang, X., Hua, S., et al. (2014). Parity-time symmetry and variable optical isolation in active-passive-coupled microresonators. *Nat. Photonics* 8, 524-529.
147. Krasnok, A., Baranov, D., Li, H., et al. (2019). Anomalies in light scattering. *Adv. Opt. Photon* 11, 892-951.
148. Zhou, J., Zhang, B., Xiao, W., et al. (2019). Nonlinear parity-time-symmetric model for constant efficiency wireless power transfer: Application to a drone-in-flight wireless charging platform. *IEEE Trans. Ind. Electron.* 66, 4097-4107.
149. Assaworrorarit, S., and Fan, S. (2020). Robust and efficient wireless power transfer using a switch-mode implementation of a nonlinear parity-time symmetric circuit. *Nat. Electron.* 3, 273-279.
150. Sakhdari, M., Hajizadegan, M., and Chen, P.-Y. (2020). Robust extended-range wireless power transfer using a higher-order PT-symmetric platform. *Phys. Rev. Res.* 2, 013152.
151. Ra'Di, Y., Chowkwale, B., Valagiannopoulos, C., et al. (2018). On-site wireless power generation. *IEEE Trans. Antenn. Propag.* 66, 4260-4268.
152. Liu, F., Chowkwale, B., Jayathurathnage, P., et al. (2019). Pulsed self-oscillating nonlinear systems for robust wireless power transfer. *Phys. Rev. Appl.* 12, 054040.
153. Liu, Y., Hao, T., Li, W., et al. (2018). Observation of parity-time symmetry in microwave photonics. *Light Sci. Appl.* 7, 38.
154. Chen, W., Kaya Özdemir, Ş., Zhao, G., et al. (2017). Exceptional points enhance sensing in an optical microcavity. *Nature* 548, 192-196.
155. Peng, B., Özdemir, Ş.K., Lei, F., et al. (2014). Parity-time-symmetric whispering-gallery microcavities. *Nat. Phys.* 10, 394-398.
156. Yao, R., Lee, C.S., Podolskiy, V., et al. (2019). Electrically injected parity time-symmetric single transverse-mode lasers. *Laser Photon. Rev.* 13, 1800154.
157. Longhi, S. (2010). PT-symmetric laser absorber. *Phys. Rev.* 82, 031801.
158. Chen, P.-Y., Sakhdari, M., Hajizadegan, M., et al. (2018). Generalized parity-time symmetry condition for enhanced sensor telemetry. *Nat. Electron.* 1, 297-304.
159. Smith, D.R., Pendry, J.B., and Wiltshire, M.C.K. (2004). Metamaterials and negative refractive index. *Science* 305, 788-792.
160. Huang, Y. (2021). *Antennas: From Theory to Practice* (John Wiley & Sons).
161. Zhou, J., Zhang, P., Han, J., et al. (2022). Metamaterials and metasurfaces for wireless power transfer and energy harvesting. *Proc. IEEE* 110, 31-55.

162. Pendry, J.B. (2000). Negative refraction makes a perfect lens. *Phys. Rev. Lett.* 85, 3966-3969.
163. Lee, W., and Yoon, Y.-K. (2020). Wireless power transfer systems using meta-materials: A review. *IEEE Access* 8, 147930-147947.
164. Wang, B., Teo, K.H., Nishino, T., et al. (2011). Experiments on wireless power transfer with metamaterials. *Appl. Phys. Lett.* 98.
165. Urzhumov, Y., and Smith, D.R. (2011). Metamaterial-enhanced coupling between magnetic dipoles for efficient wireless power transfer. *Phys. Rev. B* 83, 205114.
166. Younesiraad, H., and Bemani, M. (2018). Analysis of coupling between magnetic dipoles enhanced by metasurfaces for wireless power transfer efficiency improvement. *Sci. Rep.* 8, 14865.
167. Cho, Y., Lee, S., Kim, D.-H., et al. (2018). Thin hybrid metamaterial slab with negative and zero permeability for high efficiency and low electromagnetic field in wireless power transfer systems. *IEEE Trans. Electromagn. C.* 60, 1001-1009.
168. Das, R., Basir, A., and Yoo, H. (2019). A metamaterial-coupled wireless power transfer system based on cubic high-dielectric resonators. *IEEE Trans. Ind. Electron.* 66, 7397-7406.
169. Lu, C., Rong, C., Huang, X., et al. (2019). Investigation of negative and near-zero permeability metamaterials for increased efficiency and reduced electromagnetic field leakage in a wireless power transfer system. *IEEE Trans. Electromagn. C.* 61, 1438-1446.
170. Lu, C., Huang, X., Tao, X., et al. (2020). Comprehensive analysis of side-placed metamaterials in wireless power transfer system. *IEEE Access* 8, 152900-152908.
171. Maji, S., Sinha, S., Regensburger, B., et al. (2020). Reduced-fringing-field multi-MHz capacitive wireless power transfer system utilizing a metasurface-based coupler. In Paper Presented at: 2020 IEEE 21st Workshop on Control and Modeling for Power Electronics (COMPEL) (IEEE).
172. Ranaweera, A.L.A.K., Pham, T.S., Bui, H.N., et al. (2019). An active metasurface for field-localizing wireless power transfer using dynamically reconfigurable cavities. *Sci. Rep.* 9, 11735.
173. Li, L., Liu, H., Zhang, H., et al. (2018). Efficient wireless power transfer system integrating with metasurface for biological applications. *IEEE Trans. Ind. Electron.* 65, 3230-3239.
174. Landy, N.I., Sajuyigbe, S., Mock, J.J., et al. (2008). Perfect metamaterial absorber. *Phys. Rev. Lett.* 100, 207402.
175. Shinohara, N. (2021). History and innovation of wireless power transfer via microwaves. *IEEE J. Microw.* 1, 218-228.
176. Wu, X., Xia, X., Tian, J., et al. (2016). Broadband reflective metasurface for focusing underwater ultrasonic waves with linearly tunable focal length. *Appl. Phys. Lett.* 108.
177. Yu, S., Liu, H., and Li, L. (2019). Design of near-field focused metasurface for high-efficient wireless power transfer with multifocus characteristics. *IEEE Trans. Ind. Electron.* 66, 3993-4002.
178. Van Wagoningen, D., and Staring, T. (2010). The Qi wireless power standard. In Paper Presented at: Proceedings of 14th International Power Electronics and Motion Control Conference EPE-PEMC 2010 (IEEE).
179. Airfuel Standard Consortium Website. <https://airfuel.org/>.
180. Au, E. (2021). New IEEE Vehicular Technology Society Standards Initiatives [Standards]. *IEEE Veh. Technol. Mag.* 16, 98.
181. Bhusal, R., and Moh, S. (2014). Qualitative and quantitative comparison of IEEE 802.15.3c and IEEE 802.11ad for multi-gbps local communications. *Wireless Pers. Commun.* 75, 2135-2149.
182. Commission, I.E. (2019). Electric Vehicle Wireless Power Transfer (WPT) Systems—Part 1: General Requirements (International Electrotechnical Commission).
183. Schneider, J. (2013). SAE J2954 Overview and Path Forward (SAE International).
184. Regensburger, B., Sinha, S., Kumar, A., et al. (2022). High-performance multi-MHz capacitive wireless power transfer system for EV charging utilizing interleaved-foil coupled inductors. *IEEE J. Sel. Topics Pow. Electron.* 10, 35-51.
185. Dai, J., and Ludois, D.C. (2016). Capacitive power transfer through a conformal bumper for electric vehicle charging. *IEEE J. Sel. Topics Pow. Electron.* 4, 1015-1025.
186. Madawala, U.K., and Thrimawithana, D.J. (2011). A bidirectional inductive power interface for electric vehicles in V2G systems. *IEEE Trans. Ind. Electron.* 58, 4789-4796.
187. Budhia, M., Covic, G.A., and Boys, J.T. (2011). Design and optimization of circular magnetic structures for lumped inductive power transfer systems. *IEEE Trans. Power Electron.* 26, 3096-3108.
188. Kan, T., Nguyen, T.-D., White, J.C., et al. (2017). A new integration method for an electric vehicle wireless charging system using LCC compensation topology: Analysis and design. *IEEE Trans. Power Electron.* 32, 1638-1650.
189. Zhang, W., White, J.C., Abraham, A.M., et al. (2015). Loosely Coupled Transformer Structure and Interoperability Study for EV Wireless Charging Systems. *IEEE Trans. Power Electron.* 30, 6356-6367.
190. Lu, J., Zhu, G., and Mi, C.C. (2022). Foreign Object Detection in Wireless Power Transfer Systems. *IEEE Trans. Ind. Appl.* 58, 1340-1354.
191. Jeong, S.Y., Kwak, H.G., Jang, G.C., et al. (2016). Living object detection system based on comb pattern capacitive sensor for wireless EV chargers. In Paper Presented at: 2016 IEEE 2nd Annual Southern Power Electronics Conference (SPEC) (IEEE).
192. Choi, S.Y., Gu, B.W., Jeong, S.Y., et al. (2015). Advances in wireless power transfer systems for roadway-powered electric vehicles. *IEEE J. Sel. Topics Power Electron.* 3, 18-36.
193. Kim, J., Kim, J., Kong, S., et al. (2013). Coil design and shielding methods for a magnetic resonant wireless power transfer system. *Proc. IEEE* 101, 1332-1342.
194. Zhou, S., and Chris Mi, C. (2016). Multi-Paralleled LCC Reactive Power Compensation Networks and Their Tuning Method for Electric Vehicle Dynamic Wireless Charging. *IEEE Trans. Ind. Electron.* 63, 6546-6556.
195. Shladover, S.E. (1988). Systems engineering of the roadway powered electric vehicle technology. In Paper Presented at: INTERNATIONAL ELECTRIC VEHICLE SYMPOSIUM (9TH).
196. Systems Control Technology, I. (1994). Roadway Powered Electric Vehicle Project Track Construction and Testing Program Phase 3D. California PATH Program, Inst Transportation Studies (University of California).
197. Cirimele, V., Diana, M., Bellotti, F., et al. (2020). The fabric ICT platform for managing wireless dynamic charging road lanes. *IEEE Trans. Veh. Technol.* 69, 2501-2512.
198. Deng, Z., Hu, H., Su, Y., et al. (2023). Design of a 60kW EV Dynamic Wireless Power Transfer System with Dual Transmitters and Dual Receivers. *IEEE J. Sel. Topics Power Electron.* 12, 316-327.
199. Kim, J.H., Lee, B.-S., Lee, J.-H., et al. (2015). Development of 1-MW inductive power transfer system for a high-speed train. *IEEE Trans. Ind. Electron.* 62, 6242-6250.
200. Ukita, K., Kashiwagi, T., Sakamoto, Y., et al. (2015). Evaluation of a non-contact power supply system with a figure-of-eight coil for railway vehicles. In Paper Presented at: 2015 IEEE PELS Workshop on Emerging Technologies: Wireless Power (2015 WoW) (IEEE).
201. Wang, Z., Cui, S., Han, S., et al. (2018). A novel magnetic coupling mechanism for dynamic wireless charging system for electric vehicles. *IEEE Trans. Veh. Technol.* 67, 124-133.
202. Park, C., Lee, S., Jeong, S.Y., et al. (2015). Uniform Power I-Type Inductive Power Transfer System With *Power Supply Rails for On-Line Electric Vehicles*. *IEEE Trans. Power Electron.* 30, 6446-6455.
203. Gao, X., Dong, S., Cui, S., et al. (2021). Unbalanced reflected impedances and compensation of TS dynamic wireless charging system. *IEEE Trans. Ind. Electron.* 68, 10378-10387.
204. Miller, J.M., Onar, O.C., White, C., et al. (2014). Demonstrating dynamic wireless charging of an electric vehicle: The benefit of electrochemical capacitor smoothing. *IEEE Power Energy Mag.* 1, 12-24.
205. Cirimele, V., Diana, M., El Sayed, N., et al. (2014). An innovative next generation E-mobility infrastructure: The eCo-FEV project. In Paper Presented at: 2014 IEEE International Electric Vehicle Conference (IEVC) (IEEE).

206. Tavakoli, R., and Pantic, Z. (2018). Analysis, design, and demonstration of a 25-kW dynamic wireless charging system for roadway electric vehicles. *IEEE J. Sel. Topics Power Electron.* 6, 1378-1393.
207. Zhang, Z., Pang, H., Lee, C.H., et al. (2017). Comparative analysis and optimization of dynamic charging coils for roadway-powered electric vehicles. *IEEE Trans. Magn.* 53, 1-6.
208. Song, B., Dong, S., Li, Y., et al. (2020). A dual-layer receiver with a low aspect ratio and a reduced output fluctuation for EV dynamic wireless charging. *IEEE Trans. Power Electron.* 35, 10338-10351.
209. Hui, S.Y. (2013). Planar wireless charging technology for portable electronic products and Qi. *Proc. IEEE* 101, 1290-1301.
210. Hui, S., and Ho, W. (2005). A new generation of universal contactless battery charging platform for portable consumer electronic equipment. *IEEE Trans. Power Electron.* 20, 620-627.
211. Zhang, Y., Chen, S., Li, X., et al. (2022). Design methodology of free-positioning nonoverlapping wireless charging for consumer electronics based on antiparallel windings. *IEEE Trans. Ind. Electron.* 69, 825-834.
212. Smirnov, P., Koreshin, E., Baranov, G., et al. (2023). Free-Positioning Multi-Receiver Wireless Power Transfer System Based on Metasurface. In Paper Presented at: 2023 IEEE MTT-S International Wireless Symposium (IWS) (IEEE).
213. Ng, W.M., Zhang, C., Lin, D., et al. (2014). Two-and three-dimensional omnidirectional wireless power transfer. *IEEE Trans. Power Electron.* 29, 4470-4474.
214. Sasatani, T., Sample, A.P., and Kawahara, Y. (2021). Room-scale magnetoquasistatic wireless power transfer using a cavity-based multimode resonator. *Nat. Electron.* 4, 689-697.
215. Li, T., Yuan, Y., Xiao, Z., et al. (2023). Large space Wireless Power Transfer System that Meets Human Electromagnetic Safety Limits. In Paper Presented at: 2023 IEEE Wireless Power Technology Conference and Expo (WPTCE) (IEEE).
216. Wang, W., Zhang, Q., Lin, H., et al. (2019). Wireless energy transmission channel modeling in resonant beam charging for IoT devices. *IEEE Internet Things J.* 6, 3976-3986.
217. Olivo, J., Carrara, S., and De Micheli, G. (2011). Energy harvesting and remote powering for implantable biosensors. *IEEE Sensor. J.* 11, 1573-1586.
218. Chen, H., Liu, M., Hao, W., et al. (2009). Low-power circuits for the bidirectional wireless monitoring system of the orthopedic implants. *IEEE Trans. Biomed. Circuits Syst.* 3, 437-443.
219. Dinis, H., and Mendes, P.M. (2021). A comprehensive review of powering methods used in state-of-the-art miniaturized implantable electronic devices. *Biosens. Bioelectron.* 172, 112781.
220. Ibrahim, A., and Kiani, M. (2016). A figure-of-merit for design and optimization of inductive power transmission links for millimeter-sized biomedical implants. *IEEE Trans. Biomed. Circuits Syst.* 10, 1100-1111.
221. Xu, D., Zhang, Q., and Li, X. (2020). Implantable magnetic resonance wireless power transfer system based on 3D flexible coils. *Sustainability* 12, 4149.
222. Mirbozorgi, S.A., Yeon, P., and Ghovanloo, M. (2017). Robust wireless power transmission to mm-sized free-floating distributed implants. *IEEE Trans. Biomed. Circuits Syst.* 11, 692-702.
223. Abid, A., O'Brien, J.M., Bense, T., et al. (2017). Wireless power transfer to millimeter-sized gastrointestinal electronics validated in a swine model. *Sci. Rep.* 7, 46745.
224. Sedehi, R., Budgett, D., Jiang, J., et al. (2021). A wireless power method for deeply implanted biomedical devices via capacitively coupled conductive power transfer. *IEEE Trans. Power Electron.* 36, 1870-1882.
225. Agarwal, K., Jegadeesan, R., Guo, Y.-X., et al. (2017). Wireless power transfer strategies for implantable bioelectronics. *IEEE Rev. Biomed. Eng.* 10, 136-161.
226. Galinina, O., Tabassum, H., Mikhaylov, K., et al. (2016). On feasibility of 5G-grade dedicated RF charging technology for wireless-powered wearables. *IEEE Wireless Commun.* 23, 28-37.
227. Yan, Z., Zhang, Y., Kan, T., et al. (2019). Frequency optimization of a loosely coupled underwater wireless power transfer system considering eddy current loss. *IEEE Trans. Ind. Electron.* 66, 3468-3476.
228. Kan, T., Zhang, Y., Yan, Z., et al. (2018). A rotation-resilient wireless charging system for lightweight autonomous underwater vehicles. *IEEE Trans. Veh. Technol.* 67, 6935-6942.
229. Hasaba, R., Okamoto, K., Kawata, S., et al. (2019). Magnetic resonance wireless power transfer over 10 m with multiple coils immersed in seawater. *IEEE Trans. Microw. Theor. Tech.* 67, 4505-4513.
230. Lin, M., Lin, R., Yang, C., et al. (2022). Docking to an underwater suspended charging station: Systematic design and experimental tests. *Ocean Eng.* 249, 110766.
231. Zhang, H., and Lu, F. (2020). Insulated coupler structure design for the long-distance freshwater capacitive power transfer. *IEEE Trans. Ind. Inf.* 16, 5191-5201.
232. Tamura, M., Naka, Y., Murai, K., et al. (2018). Design of a capacitive wireless power transfer system for operation in fresh water. *IEEE Trans. Microw. Theor. Tech.* 66, 5873-5884.
233. Rong, E., Sun, P., Qiao, K., et al. (2023). Six-Plate and Hybrid-Dielectric Capacitive Coupler for Underwater Wireless Power Transfer. *IEEE Trans. Power Electron.* 39, 2867-2881.
234. Ji, L., Ge, F., and Zhang, C. (2023). Design of wireless power transmission coupling structure based on rotary steerable drilling. *IEEE Trans. Power Electron.* <https://doi.org/10.1109/TPEL.2023.3319577>.
235. Song, K., Ma, B., Yang, G., et al. (2019). A rotation-lightweight wireless power transfer system for solar wing driving. *IEEE Trans. Power Electron.* 34, 8816-8830.
236. Wang, L., Li, J., Chen, H., et al. (2022). Radial-flux rotational wireless power transfer system with rotor state identification. *IEEE Trans. Power Electron.* 37, 6206-6216.
237. Mou, X., Gladwin, D., Jiang, J., et al. (2022). Near-Field Wireless Power Transfer Technology for Unmanned Aerial Vehicles: A Systematical Review. *IEEE J Sel Topics Ind Electron* 4, 147-158.
238. Brown, W., Mims, J., and Heenan, N. (1966). An experimental microwave-powered helicopter. In Paper Presented at: 1958 IRE International Convention Record (IEEE).
239. Matsumoto, H. (2002). Research on solar power satellites and microwave power transmission in Japan. *IEEE Microw. Mag.* 3, 36-45.
240. Sasaki, S., Tanaka, K., and Maki, K.-i. (2013). Microwave power transmission technologies for solar power satellites. *Proc. IEEE* 101, 1438-1447.
241. <https://www.kenkai.jaxa.jp/research/ssps/150301.html>.
242. Strassner, B., and Chang, K. (2013). Microwave power transmission: Historical milestones and system components. *Proc. IEEE* 101, 1379-1396.
243. Liu, H., Zhang, Y., Hu, Y., et al. (2021). Laser Power Transmission and Its Application in Laser-Powered Electrical Motor Drive: A Review. *Pow Electron Drives* 6, 167-184.
244. Zhang, J., Cui, S., Bie, Z., et al. (2024). The state-of-the-arts of underwater wireless power transfer: A comprehensive review and new perspectives. *Renew Sust Energy Rev* 189, 113910.
245. Li, S., Duan, H., Xia, J., et al. (2022). Analysis and Case Study of National Economic Evaluation of Expressway Dynamic Wireless Charging. *Energies* 15, 6924.
246. Rim, C.T. (2013). Trend of roadway powered electric vehicle technology. In *Magazine of the Korean Institute of Power Electronics (KIPE)*, 78, pp. 45-51.
247. Jeong, S., Jang, Y.J., and Kum, D. (2015). Economic analysis of the dynamic charging electric vehicle. *IEEE Trans. Power Electron.* 30, 6368-6377.
248. Li, C., Dong, X., Cipcigan, L.M., et al. (2023). Economic viability of dynamic wireless charging technology for private EVs. *IEEE Trans. Transp. Electrification* 9, 1845-1856.
249. Lazzaroni, P., Cirimele, V., and Canova, A. (2021). Economic and environmental sustainability of Dynamic Wireless Power Transfer for electric vehicles supporting reduction of local air pollutant emissions. *Renew Sust Energy Rev* 138, 110537.
250. International Commission on Non-Ionizing Radiation Protection ICNIRP (2020). Guidelines for limiting exposure to electromagnetic fields (100 kHz to 300 GHz). *Health Phys.* 118, 483-524.

251. Bailey, W.H., Harrington, T., Hirata, A., et al. (2019). Synopsis of IEEE Std C95.1™-2019 "IEEE standard for safety levels with respect to human exposure to electric, magnetic, and electromagnetic fields, 0 Hz to 300 GHz". IEEE Access 7, 171346-171356.
252. Clegg, F.M., Sears, M., Friesen, M., et al. (2020). Building science and radiofrequency radiation: What makes smart and healthy buildings. Build. Environ. 176, 106324.
253. Besnoff, J., Abbasi, M., and Ricketts, D.S. (2017). Ultrahigh-data-rate communication and efficient wireless power transfer at 13.56 MHz. IEEE Antenn. Wireless Propag. Lett. 16, 2634-2637.
254. Li, X., Tang, C., Dai, X., et al. (2018). An inductive and capacitive combined parallel transmission of power and data for wireless power transfer systems. IEEE Trans. Power Electron. 33, 4980-4991.